Stony Brook University

Variants of Monoacylglycerol Lipase (MAGL) and an Assessment of a Spectrophotometric Assay for MAGL Activity

A Dissertation Presented

by

Nadine Martina Ulloa

to

The Graduate School

in Partial Fulfillment of the

Requirements

for the Degree of

Doctor of Philosophy

in

Genetics

Stony Brook University

August 2011

Stony Brook University

The Graduate School

Nadine Martina Ulloa

We, the dissertation committee for the above candidate for the

Doctor of Philosophy degree, hereby recommend

acceptance of this dissertation.

Dale G. Deutsch, Ph.D. – Dissertation Advisor
Professor, Department of Biochemistry and Cell Biology

Berhane Ghebrehiwet, DVM, Ph.D. - Chairperson of Defense
Professor, Department of Medicine

Stella E. Tsirka, Ph.D.
Professor, Department of Pharmacological Sciences

Carol A. Carter, Ph.D.
Professor, Department of Molecular Genetics and Microbiology

Marian J. Evinger, Ph.D. – Outside Member of Defense
Associate Professor, Department of Pediatrics, Stony Brook University

This dissertation is accepted by the Graduate School

Lawrence Martin
Dean of the Graduate School

Abstract of the Dissertation

Variants of Monoacylglycerol Lipase (MAGL) and an Assessment of a Spectrophotometric Assay for MAGL Activity

by

Nadine Martina Ulloa

Doctor of Philosophy

in

Genetics

Stony Brook University

2011

Monoacylglycerol lipase (MAGL) is the principal enzyme responsible for hydrolysis of the endocannabinoid, 2-arachidonylglycerol (2-AG). MAGL is universally expressed as a ~33 kDa protein. However, a ~35 kDa form of MAGL is also expressed in brain and testes while being absent in other tissues. Interestingly, the MAGL mRNA sequence contains two putative translation initiation sites upstream of the start codon originally used for MAGL cloning, which may explain the ~35 kDa form. Examination of whole mouse brain and brain region cDNA revealed the presence of three MAGL transcript sequences. These sequences were isolated and characterized in neuronal and non-neuronal cell lines. It was determined that all three constructs are enzymatically active, are expressed by all cell lines, and have similar sub-cellular localizations. These data indicate that despite their differing N-termini peptide sequences, these MAGL variants possess redundancy in their activity and cellular trafficking. Since the characteristics of the MAGL variants examined did not differ between non-neuronal and neuronal cell lines, the expression of ~35kDa protein may be a result of other modes of protein regulation such as protein interactions only stimulated by incubation with 2-AG or post-translational modifications.

MAGL activity is usually measured by costly radiometric or time-consuming mass spectrometric assays. An assessment of a spectrophotometric assay was carried out to determine its usefulness as an alternative method. MAGL obtained from transiently transfected COS-7 cells was incubated with arachidonoyl-1-thio-glycerol, a thioester-containing analog of 2-AG, which results in the release of a thiolate ion that has measurable absorbance at 412 nm. This spectrophotometric assay was used to measure MAGL activity and measure inhibition by the sulfhydryl inhibitor, *N*-arachidonyl maleimide (NAM). Most results obtained were comparable to those reported in previous studies. The spectrophotometric assay, therefore, is a useful tool for general purposes such as initial high-throughput screening of inhibitors.

Dedication

In memory of my wonderful grandmothers

Juana Jimenez and Ana Delia Lopez

I would not be here without their perseverance

Table of Contents

List of Figures

List of Abbreviations

2-AG	2-arachidonylglycerol
2-OG	2-oleoylglycerol
A-1-TG	arachidonyl-1-thio-glycerol
ABHD6	alpha/beta hydrolase domain-containing 6
ABHD12	alpha/beta hydrolase domain-containing 12
AEA	*N*-arachidonylethanolamide / anandamide
Bcl-2	B-cell lymphoma 2
BSA	bovine serum albumin
cAMP	cyclic adenosine monophosphate
CB1	cannabinoid receptor 1
CB2	cannabinoid receptor 2
DTNB	5,5'-dithiobis(2-nitrobenzoic acid)
DGLα	diacylglycerol lipase alpha
DSE	depolarization-induced suppression of excitation
DSI	depolarization-induced suppression of inhibition
ER	endoplasmic reticulum
ERK1/2	extracellular signal regulated kinase 1/2
FAAH	fatty acid amide hydrolase
GABA	gamma-aminobutyric acid
GFP	green fluorescent protein
GPCR	G-protein coupled receptor
JNK	c-Jun N-terminal kinase
LTD	long-term depression
MAFP	methylarachidonylfluorophosphonate
MAGL	monoacylglycerol lipase
MAPK	mitogen activated protein kinase
NAM	*N*-arachidonyl maleimide
NMDA	N-methyl-D-apartic acid
PI3K	phosphatidylinositol-3-kinase
PLCβ	phospholipase C beta
PM-GFP	plasma membrane – green fluorescent protein
PNGaseF	N-glycosidase F
Raf-1	Ras activated factor-1
THC	Δ^9-tetrahydrocannabinol
TNB	2-nitro-5-mercaptobenzoic acid
UTR	untranslated region

Acknowledgments

First of all, I would like to thank my advisor, Dr. Dale Deutsch. Joining his lab was unexpected, but worked out really well. He has really allowed me to become an independent thinker which, I think, will be one of the greatest assets I've gained in graduate school and will continue to benefit me in my career. He also pushed me when I didn't want to be pushed, which, at the time, did not make me very happy, but I got so much done that wouldn't have gotten done as quickly otherwise! I would also like to thank him and his wife, Dr. Lou Deutsch, for showing me so much kindness, caring, and worrying about my well-being during the highly stressful time I experienced while writing this dissertation.

I would like to thank my thesis committee members: Dr. Stella Tsirka, Dr. Berhane Ghebrehiwet, Dr. Carol Carter, and Dr. Marian Evinger for their great ideas for experiments, constructive criticisms, and approachability. I would also like to thank them for being so understanding when I had to re-schedule my defense!

I would like to thank my lab mate, Dr. Martin Kaczocha, for his help with ideas for and troubleshooting of experiments. His vast knowledge of the endocannabinoid field just amazes me. He answers so many of my questions - his help was indispensable my first few years in the lab. I'd also like to thank him for great non-scientific conversations and just making my time in the lab a lot more fun than it would have been otherwise. I could do without his April Fool's jokes though! Also thanks to our lab tech, Jing Sun, for helping with our mouse project from which data is, unfortunately, not presented in this dissertation.

I'd like to thank Dr. Deborah Brown and the members of her lab for helping me troubleshoot experiments, giving me opinions on data, and giving me an extra plate of cells when I needed it! Thanks to Kate Bell and the Genetics Program for making administrative aspects of graduate school not inconvenient.

Thank you to my wonderful classmates for their support and making graduate school a lot more bearable! I'd especially like to thank my classmates, Dr. Joseph Lachance, Dr. Azad Gucwa, and Dr. Kinga Hosszu for lending an ear to so many of the

science and non-science issues I dealt with during our time at Stony Brook. Where would I be without their encouragement!

Of course, so many thanks go to my family for their endless love, support, and encouragement: my parents, José & Dulce, for instilling in me the values I cherish, my sister, Vianka, for constant caring and long phone conversations, my brother, Alvin, for making me laugh so much, and my nephews who have brought so much more love and joy to my life. Last, but not least, I'd like to thank my wonderful fiancé, Pieter, whom without his unconditional love and eternal optimism I would be lost.

Chapter 3 of this dissertation was reprinted/reused with kind permission from Springer+Business Media: Ulloa, N.M., and D.G. Deutsch. (2010) Assessment of a spectrophotometric assay for monoacylglycerol lipase activity. *AAPS J.*12:197-201.

Publications

Tsuboi K., Okamoto Y., Ikematsu N., Inoue M., Shimizu Y., Uyama T., Wang J., Deutsch, D.G., Burns M.P., **Ulloa N.M.**, Tokumura A., and N. Ueda. (2011) Enzymatic formation of N-acylethanolamines from N-acylethanolamine plasmalogen through N-acylphosphatidylethanolamine-hydrolyzing phospholipase D-dependent and –independent pathways. *Biochim. Biophys. Acta.* (epub ahead of print).

Howlett, A.C., Reggio, P.H., Childers, S.R., Hampson, R.E., **Ulloa, N.M.**, and D.G. Deutsch (2011) Endocannabinoid tone versus constitutive activity of cannabinoid receptors. *Br. J. Pharmacol.* 163:1329-1343.

Ulloa, N.M., and D.G. Deutsch. (2010) Assessment of a spectrophotometric assay for monoacylglycerol lipase activity. *AAPS J.*12:197-201.

Chapter 1

The Endocannabinoid System

Summary

Endocannabinoids are neuromodulatory lipids that are pharmacologically related to the psychoactive component of the cannabis plant. They modulate synaptic plasticity by acting as retrograde messengers and inhibiting excitatory and inhibitory neurons. Endocannabinoids are known to play roles in a variety of physiological functions and therefore are attractive targets for drugs designed for the treatment of many ailments and illnesses.

Cannabinoid receptors

The psychotropic effects and therapeutic properties of marijuana (*Cannabis sativa*) were known for millennia before Δ^9-tetrahydrocannabinol (THC), was isolated (Gaoni, 1964). Studies administering constituents of marijuana, termed "phytocannabinoids", to adult rhesus monkeys determined that animals given THC or a mixture of THC and other phytocannabinoids displayed behavioral changes, such as loss of movement, apathy, and drowsiness, previously associated with marijuana use (Mechoulam et al., 1970). Animals given non-THC-containing mixtures of phytocannabinoids did not exhibit any of these behaviors.

THC structure elucidation generated interest in synthesizing non-psychotropic cannabinoids that retain their therapeutic properties. The analgesic, CP-55,940, is one such compound. CP-55,940 was shown to inhibit adenylate cyclase and require guanine and Ca^{2+} for binding in rat membrane preparations and neuronal cell lines (Devane et al., 1988). These are indicators for binding to a G-protein coupled receptor (GPCR). Indeed, a cDNA sequence cloned from a rat membrane cortical cDNA library

encoding a 473-amino acid GPCR exhibited such characteristics and was named cannabinoid receptor 1 (CB1) (Matsuda et al., 1990). Mouse and human homologs of CB1 were identified shortly thereafter (Chakrabarti et al., 1995; Gerard et al., 1990). CB1 is expressed throughout the brain at various levels in specific subpopulations of neurons (Mailleux et al., 1992; Matsuda et al., 1993). It localizes to presynaptic axon terminals at both excitatory and inhibitory synapses (Kano et al., 2009). CB1 mRNA can be detected in several peripheral organs including heart, lung, and small intestines (Thakur et al., 2005). Another cannabinoid receptor, cannabinoid receptor 2 (CB2), was cloned from HL60, a human leukemic cell line. It is also a GPCR and shares only 44% sequence identity with CB1 (Munro et al., 1993). It is highly abundant in cells of immunologic origin including macrophages, natural killer cells, T lymphocytes and B cells (Berdyshev, 2000).

Endocannabinoids

The identification of the CB1 receptor led to the belief that there were likely endogenous ligands for CB1. Indeed, the arachidonic acid-containing (C20:4) compounds, *N*-arachidonylethanolamide (anandamide, AEA), was isolated from pig brain fractions when it displaced the radio-labeled synthetic cannabinoid, HU-243, from CB1 (Devane et al., 1992). This “endocannabinoid” is a partial agonist at both the CB1 and CB2 receptors (Sugiura et al., 2002). Studies measuring the total amounts of anandamide in the brain and peripheral tissues generally report levels of ~0.5-165 pmol/g tissue with the exceptions being the mouse uterus (~2-21 nmol/g tissue) and human brain (50 nmol/g tissue) (Sugiura et al., 2002). Another endocannabinoid, 2-arachidonylglycerol (2-AG) was isolated from the canine gut and rat brain using the same methods that were used to isolate AEA (Mechoulam et al., 1995; Sugiura et al., 1995). It is a full agonist at both the CB1 and CB2 receptors. It is relatively abundant in the brain (~1-4 nmol/g tissue for rat brain) and peripheral tissues compared to anandamide (Sugiura et al., 2002). Other putative endocannabinoids including docosatetraenoyl ethanolamide, 2-arachidonylglycerol ether (noladin ether), *O*-

arachidonoylethanolamine (virodhamine), and *N*-arachidonoyldopamine have been isolated from brain tissue (Walker and Huang, 2002). They all contain an arachidonic acid acyl chain and display varying degrees of agonism at CB1 and CB2 receptors. However, it is unclear if these compounds are involved in intercellular signaling pathways *in vivo* (Walker and Huang, 2002).

Endocannabinoid signaling in the central nervous system

Endocannabinoids are retrograde neurotransmitters (Kreitzer and Regehr, 2001; Maejima et al., 2001; Ohno-Shosaku et al., 2001; Wilson and Nicoll, 2001). They are synthesized in postsynaptic neurons, traverse the synaptic cleft and bind to CB1 receptors in the presynaptic neuron. Unlike "classical neurotransmitters" such as acetylcholine, glutamate, or γ-aminobutyric acid (GABA), the hydrophobic nature of endocannabinoids does not allow for their storage in synaptic vesicles. Therefore, endocannabinoids are thought to be synthesized "on demand". For example, 2-AG synthesis may be stimulated through a couple of mechanisms. One mode of 2-AG synthesis results from a high influx of calcium stimulating an as-of-yet uncharacterized enzyme to produce diacylglycerol from an arachidonic acid-containing membrane phospholipid. Diacylglycerol is then hydrolyzed by diacylglycerol lipase alpha (DGLα) producing 2-AG (Gao et al., 2010; Tanimura et al., 2010). Another pathway through which 2-AG is synthesized involves stimulation of a $G_{q/11}$PCR by an influx of calcium which then activates phospholipase C beta (PLCβ) via the G-protein β/γ subunit (Hashimotodani et al., 2005; Maejima et al., 2005). PLCβ produces diacylglycerol lipase, which is subsequently hydrolyzed by DGLα to form 2-AG. The mechanism by which endocannabinoids cross the synaptic cleft is unknown.

Binding of CB1 receptors by endocannabinoids leads to several intracellular changes in the presynaptic neuron. One of the first reported effects of CB1 receptor binding was inhibition of adenylate cyclase (Howlett et al., 1988). This would indicate coupling of the CB1 receptor to the $G_{i/o}$ subtype of G proteins. CB1 receptor activation decreases intracellular calcium and potassium stores via inhibition of voltage-gated

calcium channels and activation of inwardly-rectifying potassium channels respectively (Turu and Hunyady, 2010). Several protein kinases including mitogen activated protein kinase (MAPK), ERK1/2, JNK, and PI3K, are also activated via the CB1 receptor (Turu and Hunyady, 2010). These intracellular changes in concert result in inhibition of neurotransmitter release from the presynaptic neuron. Inhibition may be transient (short-term depression) or persistent (long-term depression) and is dependent on the relative influx of calcium into the postsynaptic neuron. The increasing concentration of intracellular calcium ions (i.e. depolarization) in the postsynaptic neuron triggers one of the aforementioned pathways for 2-AG synthesis. There may be short-term depression of both excitatory (depolarization-induced suppression of excitation or DSE) and inhibitory (depolarization-induced suppression of inhibition or DSI) presynaptic neurons (Kano et al., 2009). Some evidence also indicates that long-term depression (LTD) functions similarly to short-term depression but is mediated through additional target proteins in the presynaptic neuron to sustain its own inhibition (Kano et al., 2009). Hydrolysis of 2-AG by monoacylglycerol lipase (discussed in the next chapter) in the presynaptic neuron terminates the signal.

Physiological functions of endocannabinoids

Endocannabinoids play essential roles in a variety of physiological functions. Anandamide and 2-AG are known to increase in regions of the brain known to modulate responses to pain including the amygdala, a section of the midbrain called the periacqueductal grey, an area of the brainstem called the rostral ventromedial medulla, and the dorsal horn of the spinal cord (Hohmann and Suplita, 2006). Electrical stimulation or infusion of CB1 receptor agonists into these brain regions result in endocannabinoid-mediated analgesia (Hohmann and Suplita, 2006). Antinociceptive pathways occur through endocannabinoid inhibition of presynaptic GABA and glutamate receptors as inhibition of these receptors blocks the antinociceptive affects of CB1 agonists (Hohmann and Suplita, 2006).

Endocannabinoids participate in the regulation of food intake and energy homeostasis. Anandamide and 2-AG are known to increase during fasting and decrease during food intake in regions in the brain associated with the hunger/satiety neuronal circuitry (Li et al., 2011). CB1 receptors are also known to co-localize with dopaminergic receptors that are involved in the “reward” neuronal signaling pathways (i.e. induction of feelings of pleasure and motivation) (Li et al., 2011). Additionally, endocannabinoids in peripheral organs such as the gastrointestinal tract, adipose tissue, pancreas, skeletal muscle, and liver are known to promote energy storage by increasing lipogenesis, decreasing intestinal tract motility, and reducing glucose uptake (Li et al., 2011). Endocannabinoids also seem to play a limited role in the healthy cardiovascular system, but are upregulated in cases of hypertension and impaired cardiac function (Batkai and Pacher, 2009).

Although data have emerged to the contrary, many studies have shown that anandamide and 2-AG are involved in modulating the immune system response by antagonizing inflammatory signals (Berdyshev, 2000; Fowler et al., 2010; Tanasescu and Constantinescu, 2010). Activation of cannabinoid receptors is likely to initiate this process by mainly inhibiting cAMP and activating MAPK (Berdyshev, 2000; Tanasescu and Constantinescu, 2010). Cannabinoid receptor activation dampens the inflammatory response in a variety of ways including decreasing cytokine release, changing immune cell migration and proliferation, antibody production, and decreasing nitric oxide production (Berdyshev, 2000; Fowler et al., 2010; Tanasescu and Constantinescu, 2010). As related hematopoetic-derived cells, microglia are also subjected to CB2-mediated anti-inflammatory actions and thus endocannabinoids play a neuroprotective role in brain injury (Berdyshev, 2000; Fowler et al., 2010). Endocannabinoid production is also stimulated in neurons during brain injury and can stall the effects of neurotoxicity resulting from hyperactive release of neurotransmitters such as GABA or glutamate. Additionally, a common characteristic of neurodegenerative diseases is the loss of CB1 receptor expression (Fowler et al., 2010). This further confirms the importance of endocannabinoids in neuroprotection.

Anandamide and 2-AG are found at higher levels in tumor cells than normal cells and are believed to act as tumor suppressors at the early stages of cancer. Treatment

of several cancer cell lines with CB1 receptor agonists decreased their proliferation (Pisanti and Bifulco, 2009). Endocannabinoids affect proliferation of tumor cells by inhibiting cell cycle proteins and initiating pro-apoptotic signals such as affecting the apoptotic regulator protein, Bcl2, upregulating expression of stress proteins, and activating the oncogene, Raf1 (Pisanti and Bifulco, 2009). Tumor cell migration and invasion are also inhibited by endocannabinoids. Inhibition of matrix-metalloproteinase 2 is one mechanism by which endocannabinoids prevent tumor cells from establishing new sites of metastasis (Pisanti and Bifulco, 2009).

Endocannabinoids are also associated with the regulation of cognitive function. As previously mentioned, the cannabinoid receptor interaction with dopamine receptors is part of the reward neuronal circuitry underlying addiction (Fride, 2005; Li et al., 2011). Endocannabinoids also function in modulating response to different kinds of stress (acute vs. chronic stress) (Fride, 2005). An increase in 2-AG levels in the stress response center of the brain, the hypothalamic-pituitary-adrenal axis, was found to correlate with chronic stress while the opposite was seen with acute stress (Fride, 2005). Cannabinoid receptor localization to areas of the brain associated with motor function is evidenced by ataxia experienced by marijuana users and observed in cannabinoid receptor agonist-treated mice (Fride, 2005). Their mechanism of action for motor function, however, remains unclear. There is also some evidence suggesting that the over-expression of CB1 receptors is part of the neurological basis for psychosis experienced by schizophrenics (Fride, 2005).

It is clear that the components of the endocannabinoid system are attractive targets for drug design for a variety of diseases, disorders, and ailments including pain, nausea, hypertension, neurodegenerative disorders such as multiple sclerosis and huntington's disease, cancer, addiction, depression, schizophrenia, and motor function disorders like epilepsy.

Chapter 2

Variants of Monoacylglycerol Lipase

ABSTRACT

Monoacylglycerol lipase (MAGL) is the principal enzyme responsible for hydrolysis of the endocannabinoid, 2-arachidonylglycerol (2-AG). Originally cloned from rat adipocytes, MAGL is universally expressed as a ~33 kDa protein. However, a ~35 kDa form of MAGL is also expressed in brain and testes while being absent in other tissues. Interestingly, the MAGL mRNA sequence contains two putative translation initiation sites upstream of the start codon originally used for MAGL cloning. This may explain the ~35 kDa form of MAGL since translation from these start sites would add about 1-2 kDa to the mature MAGL protein. Examination of whole mouse brain and brain region cDNA revealed the presence of three MAGL transcript sequences. These sequences were isolated, inserted into plasmids, and used in experiments to compare their enzymatic activity, protein expression, and sub-cellular localization in neuronal (N18TG2, HT22) and non-neuronal (HeLa, COS-7) cell lines. All three constructs are expressed as single proteins of expected molecular weights in neuronal and non-neuronal cell lines. Additionally, all constructs possess significant hydrolytic activity when compared to empty vector control cells, but do not significantly differ in their enzymatic activities when compared to each other. All three constructs exhibit cytosolic localization with partial to complete localization to the cytosol, plasma membrane, and endoplasmic reticulum in all cell types examined. Co-localization of different pairs of constructs showed strong co-localization with the tendency to form aggregates. It is unclear whether the sequences isolated are transcribed from MAGL DNA individually or are part of one large sequence. These data indicate that despite their differing N-termini peptide sequences, these MAGL variants possess redundancy in their activity and

cellular trafficking. Since the characteristics of the MAGL variants examined did not differ between non-neuronal and neuronal cell lines, the expression of the ~35kDa form of MAGL may be a result of other modes of protein regulation, such as post-translational modifications or stimulation by 2-AG in intact cells to initiate neuron-specific transcription/translation and/or protein interactions.

INTRODUCTION

Monoacylglycerol lipase is the principal enzyme for 2-AG hydrolysis

MAGL was first described as the enzyme that catalyzes the last step in triglyceride metabolism by hydrolyzing 2-monoacylglycerols and to a smaller extent 1(3)-monoacylglycerols to produce free fatty acids and glycerol (Fredrikson et al., 1986). It was purified from rat adipose and identified as an ~33 kDa protein (Tornqvist and Belfrage, 1976). Cloning also predicted a protein of ~33 kDa (Karlsson et al., 1997). Rat MAGL and human MAGL are 303-amino acids long and share 97% and 93% peptide sequence identity with mouse MAGL, respectively. Although MAGL does not share significant homology with any mammalian proteins, it shares 20-25% sequence identity with yeast and bacterial esterases, lysophospholipases, and haloperoxidases (Karlsson et al., 1997). Using sequence alignment with these known bacterial and yeast enzymes along with secondary structure prediction programs, it was shown that the peptide sequence and secondary structure of MAGL contained the hallmarks of an α/β-fold serine hydrolase including the characteristic catalytic triad (Karlsson et al., 1997). Site-directed mutagenesis determined that Ser-122, Asp-239, and His-269 are essential for MAGL enzymatic activity (Karlsson et al., 1997).

It was hypothesized that 2-AG hydrolysis occurred via the same enzyme that hydrolyzes anandamide, fatty acid amide hydrolase (FAAH). Although FAAH is capable of hydrolyzing both anandamide and 2-AG *in vitro*, further studies indicated that a 2-AG

hydrolase activity distinguishable from FAAH existed in the brain (Beltramo and Piomelli, 2000; Goparaju et al., 1999; Goparaju et al., 1998; Lang et al., 1999; Patricelli and Cravatt, 1999). MAGL was considered a good candidate enzyme for 2-AG hydrolysis. Northern blot analysis and *in situ* hybridization studies revealed that MAGL mRNA was found throughout the brain at varying levels (Dinh et al., 2002). MAGL mRNA levels were especially high in the cortex, cerebellum, CA1 and CA3 regions of the hippocampus, and the anterodorsal nucleus of the thalamus (Dinh et al., 2002). Upon closer examination, MAGL was found to co-localize with CB1 receptors at presynaptic axon terminals at both excitatory and inhibitory synapses. This placement in the neuron is ideal for breakdown of 2-AG (Gulyas et al., 2004; Ludanyi et al., 2011; Straiker et al., 2009; Straiker and Mackie, 2009).

Initial *in vitro* experiments sought to show that MAGL and not FAAH primarily hydrolyzes 2-AG. In one such experiment, HeLa cells transiently transfected with MAGL hydrolyzed 2-AG but not anandamide (Dinh et al., 2002). Cortical neurons over-expressing MAGL displayed a decrease in 2-AG accumulation following NMDA/cholinergic receptor activation. However, anandamide accumulation in these cells was not affected (Dinh et al., 2002). Pre-treatment of rat cerebellar membranes with the serine hydrolase inhibitor, MAFP, but not the selective FAAH inhibitor, URB597, decreased the hydrolysis of radiolabeled 2-AG (Saario et al., 2004). This confirmed that the brain contained MAGL-like activity responsible for 2-AG hydrolysis.

Further experiments inhibiting or removing endogenous MAGL showed that it plays a role in 2-AG hydrolysis *in vivo*. Absence of MAGL expression achieved either through immunodepletion or siRNA knockdown of MAGL decreased hydrolysis of exogenous 2-AG (Dinh et al., 2004). Alternatively, brains from FAAH knockout mouse retained MAGL activity (Dinh et al., 2004). An enzyme activity-based serine hydrolase screen of the mouse brain membrane proteome determined that ~85% of 2-AG hydrolysis in the brain can be attributed to MAGL (Blankman et al., 2007). Two serine hydrolases, α/β hydrolase domain-containing 6 (ABHD6) and α/β hydrolase domain-containing 12 (ABHD12), account for the remaining 2-AG hydrolytic activity in the brain (Blankman et al., 2007). Additionally, MAGL knockout mice exhibit ~10-fold increase in brain 2-AG levels compared to wild-type mice (Schlosburg et al., 2010). These

sustained elevated levels of 2-AG reduced the analgesic affects of CB1 receptor agonists, desensitized CB1 receptors, and disrupted CB1 receptor-mediated DSI and DSE (Schlosburg et al., 2010). All these data confirmed that MAGL is the principal enzyme for 2-AG hydrolysis in the central nervous system.

MAGL is a peripheral membrane protein

Studies show that the concerted activity of MAGL, ABHD6, and ABHD12 regulate 2-AG levels and signaling (Fig. 1A). Peptide sequence and secondary structure analysis of these enzymes predicted MAGL to be a peripheral membrane protein while ABHD6 and ABHD12 are integral membrane proteins (Blankman et al., 2007; Karlsson et al., 1997) Western blot analysis confirmed MAGL is expressed in both membrane and cytosolic cell fractions (Blankman et al., 2007). The majority of MAGL activity (~60 nmol/min/mg) in mouse brain is found in membrane fractions. However, cytosolic fractions also possess some MAGL activity (~5 nmol/min/mg) (Blankman et al., 2007). MAGL is expressed in neurons and absent from microglia. ABHD6 and ABHD12, on the other hand, are expressed only in membrane fractions and are sensitive to PNGaseF digestion (Blankman et al., 2007). The active site of ABHD6 is predicted to face the cytosol while the active site of ABHD12 faces the lumen/extracellular space (Blankman et al., 2007). ABHD6 is highly expressed in mouse post-synaptic neurons and astrocytes (Marrs et al., 2010). It is also expressed in the microglial cell line, BV-2, but is not in expressed in brain microglia (Marrs et al., 2010; Muccioli et al., 2007). ABHD12 is highly expressed in microglia as well as other related cell types such as osteoclasts and macrophages, but not in neurons (Fiskerstrand et al., 2010). Inhibition of ABHD6 inhibited LTD, but DSI or DSE (forms of short term depression) (Straiker and Mackie, 2009; Straiker et al., 2011). These data indicate that MAGL, ABHD6, and ABHD12 are hydrolyzing different pools of 2-AG: MAGL monitoring 2-AG levels in presynaptic neurons, ABHD6 controlling 2-AG levels at its site of generation in postsynaptic neurons, and ABHD12 monitoring 2-AG levels in microglia and similar cells in the periphery.

The solution of MAGL crystal structure confirmed that MAGL is a α/β fold protein with a central β sheet consisting of seven parallel and one anti-paralell β strand surrounded by six α helices (Bertrand et al., 2010; Labar et al., 2010; Schalk-Hihi et al., 2011). The amphitrophic helix α4 acts as a lid shielding the catalytic triad at the hydrophobic core of the enzyme (Fig. 1B). Although not confirmed experimentally, this lid is a common feature among lipases and functions to shield the hydrophobic core from the surrounding hydrophilic environment. Interaction with membranes induces a conformational change in the enzyme resulting in movement of the lid and exposure of the core to allow entry of substrate. The glycerol moiety of 2-AG enters first while the arachidonyl chain is stabilized by hydrophobic amino acids lining the channel leading to the catalytic triad (Bertrand et al., 2010; Labar et al., 2010). The glycerol moiety in the immediate hydrophilic environment of the catalytic triad is released upon catalysis and possibly exits the enzyme via a channel perpendicular to the entry channel (Bertrand et al., 2010; Labar et al., 2010). Available data is contradictory as to whether MAGL exists as a dimer or monomer *in vivo.*

MAGL isoforms

As previously mentioned, MAGL had been purified from adipose tissue and its biochemical properties characterized in an effort to understand its role in triglyceride metabolism (Fredrikson et al., 1986; Tornqvist and Belfrage, 1976). The purified protein had a molecular weight of ~33 kDa. Northern blot analysis showed MAGL mRNA as a single strand of ~4 kb in length in adipose tissue and in different brain regions (Dinh et al., 2002; Karlsson et al., 2001). However, initial western blot analysis showed that MAGL is expressed as both a ~33 and ~35 kDa protein in the brain while being expressed in most other tissues as only the ~33 kDa protein except in the testes and skeletal muscle where it is expressed as a ~30 and ~40 kDa protein respectively (Karlsson et al., 2001). Another study examining the serine hydrolase profiles of various mouse tissues showed that both brain and testes express the ~33 and ~35 kDa forms of the protein (Long et al., 2009). In the same study, administration of the

selective MAGL inhibitor, JZL184, to these mice significantly elevated 2-AG and decreased arachidonic levels in the brain. In contrast, 2-AG and arachidonic acid levels in the testes remain unchanged. 2-AG levels also increased in other peripheral organs except for lung and white adipose tissue, but not to the extent of two other monoacylglycerols, 2-palmitoylglycerol (C16:0) and 2-oleoylglycerol (C18:1) (Long et al., 2009). However, no concomitant decreases in arachidonic, palmitic, or oleic acid were observed in peripheral tissues. This study showed that MAG metabolism is tissue specific. MAGL protein expression in skeletal muscle has, to date, not been duplicated.

Analysis of mouse MAGL exon-intron organization initially determined that MAGL mRNA has seven exons and six introns (Karlsson et al., 2001). Three possible 5'-untranslated (UTR) regions 108 and 371 base pairs in length were found (Fig. 2A). The longest sequence also contained two additional translation initiation start codons upstream of the codon used in the original cloning of rat MAGL (Karlsson et al., 2001). An additional sequence with the 108 bp 5'-UTR, but a 66 bp deletion further downstream in the sequence was also discovered. Interestingly, analysis of a mouse brain cDNA library determined that six out of eight end sequence tags (ESTs) corresponded to the 371 bp 5'-UTR. The 108 bp 5'-UTR sequence was found in liver and the shortest sequence was found in kidney (Karlsson et al., 2001). The authors of the study surmised that there were unidentified exons further upstream of the sequence initially identified from which splicing could generate the differing 5'-UTR. Indeed, subsequent availability of the mouse genomic sequence confirmed that MAGL has 8 exons and 3 possible transcript isoforms (transcript variant 1 = 3.9 kb, transcript variant 2= 3.6 kb, and transcript variant 3 = 3.5 kb). Translation from the longest mRNA sequence could explain the two isoforms in the brain. Translation from the putative upstream start codons in that sequence would add about ~2 kDa to the protein. Furthermore, different 5'-UTR sequences arising from MAGL splice variants could result in differing regulation of MAGL translation in a tissue-dependent manner. This would also offer an explanation for the differences in MAG metabolism that exists between the brain and peripheral tissues (Long et al., 2009).

Characterization of expression, activity, and sub-cellular localization of these MAGL isoforms would further elucidate the regulation of MAGL in the brain compared to

other tissues. The aims of the present study are to determine 1) if the MAGL isoforms arising from the start codons in the longest MAGL mRNA sequence described above are expressed in the mouse brain 2) determine if these isoforms are present in peripheral tissues and 3) compare MAGL isoform hydrolytic activity, expression, and sub-cellular localization in neuronal and non-neuronal cell lines.

MATERIALS and METHODS

Chemicals

2-mono oleoyl glycerol racemic [1,2,3-3H] was purchased from American Radiolabeled Chemicals, Inc. (St. Louis, MO). JZL184 (4-nitrophenyl-4-(dibenzo[d][1,3]dioxol-5yl(hydroxy)methyl)piperidine-1-carboxylate was purchased from Cayman Chemical Company (Ann Arbor, MI).

mRNA extraction, cDNA analysis, and generating MAGL isoform constructs

Total mRNA was isolated from mouse tissues using the RNeasy mini kit (Qiagen) following the manufacturer's protocol. One microgram of RNA was then used to synthesize cDNA using the Quantitect Reverse Transcription Kit (Qiagen) as prescribed by the manufacturer. One microliter of cDNA was used in subsequent PCR reactions.

Primers designed to anneal against MAGL sites of translation initiation in conjunction with identical 3'-end sequence primers were used in touchdown PCR reactions to isolate the 912, 939, and 959 base pair sequences of MAGL and its larger isoforms respectively (Fig. 2B). The forward MAGL primer was 5'-GATATAGGTACC**GCCACC**ATGCCTGAGGCAAGTTCACC-3'. The forward primer for the 959 base pair sequence, arbitrarily called MAGL2, was 5'-GATAGGTACC**GCCACC**ATGCAAAAGCCAAGACTAATG-3'. The forward primer for

the 939 base pair sequence, arbitrarily called MAGL3, was 5'-GATAGGTACC**GCCACC**ATGGAAACAGGGCCTAAAGAC-3'. The reverse primer which anneals to the identical 3'-end sequences was 5'-GATATATCTCGAGTCAGGGTGGACACCCAGC-3'. The underlined nucleotides are restriction enzyme recognition sequences *KpnI* (5'-end primer) and *XhoI* (3'-end primer) while the nucleotides in bold denote the Kozak consensus sequence. PCR conditions used to isolate MAGL isoforms were the following: initial denaturing at 95°C for 5 minutes, denaturing at 95°C for 20 seconds, 58°C (-0.1°C each cycle) for 1 minute, and elongation at 72°C for 1.5 minutes (40 cycles), and final extension at 72°C for 7 minutes.

After confirmation of MAGL isoform expression, PCR reactions were purified using the MinElute PCR Purification Kit (Qiagen) and then restriction digested with *KpnI* and *XhoI* (New England Biolabs). The digested products were isolated from a 1% agarose gel using the Qiaquick Gel Extraction Kit (Qiagen) and then ligated to a *KpnI*/*XhoI*-digested pcDNA4-myc/HisA vector (Invitrogen) using the Rapid DNA Ligation Kit (Roche). The vector with insert was grown in competent DH5α *E. coli* (Invitrogen) and isolated using the QIAPrep Spin Miniprep Kit (Qiagen). Insertion of sequences into the vector was confirmed by Big Dye Terminator Sequencing (Applied Biosystems, Stony Brook HSC Sequencing Facility) over the entire open reading frame.

Analysis of brain, lung, liver, and kidney cDNA was carried out with the aforementioned corresponding MAGL isoform primer pairs using an annealing temperature gradient (54-60°C) for 40 cycles. While brain region cDNA was analyzed utilizing the same PCR conditions described above for cloning.

Myc/His-tag (all isoforms), MAGL2-myc only, and MAGL3-6xHis only constructs were generated with purified construct DNA, the MAGL isoform 5'-end primers described above and the following 3'-end primers: MycHis reverse primer 5'-GATATACTCGAGGGGTGGACACCCAGCTCC-3', Myc tag-only reverse primer 5'-ACCGGTATGCAT**T**T**A**CAGATCCTCTTC-3', and 6xHis tag-only reverse primer 5'-ACCGGTGGGTGGACACCCAGC-3'. The underlined nucleotides in the Myc/His primer are the *XhoI* recognition sequence while those underlined in the 6xHis tag-only primer are the *AgeI* recognition sequence. The bold sequences in the Myc tag-only primer

sequence are mutations that insert a stop codon after the Myc tag sequence in the construct. PCR reactions were carried out using Platinum Pfx DNA Polymerase (Invitrogen) using the following cycling conditions: denaturing at 95°C for 30 seconds, annealing for 1 minute, and elongation at 68°C for 30–60 seconds (35 cycles). A FLAG tag was added to MAGL by isolating MAGL from whole mouse brain cDNA using a primer with the FLAG octapeptide sequence (a gift from Martin Kaczocha, Deutsch Lab, Stony Brook University). Constructs were isolated and sequenced as described above. All tags were added to the C-termini of the MAGL isoforms.

Sub-cellular localization constructs

The plasmid eGFP-c1 (Clontech) was used as an empty vector and will be referred to as "GFP" in the following text. PM-GFP (a gift from Deborah Brown, Stony Brook University) is a pcDNA3 vector containing GFP modified at its N-terminus with the 10-amino acid (MGCIKSKRKD) N-terminal sequence of Lyn kinase (Chen and De Camilli, 2005). The glycine and cysteine residues in this peptide sequence are myristolated and palmitoylated respectively. This allows for localizing of GFP to the plasma membrane. The vector pDSRED2-ER (Clontech) was used as a marker for the endoplasmic reticulum (a gift from Martin Kaczocha, Deutsch Lab, Stony Brook University). It contained a calreticulin targeting sequence (MLLSVPLLLG LLGLAAADPAIYFKEQ) and an ER retention sequence (KDEL).

Tissue culture and transfection

COS-7, HeLa, and N18TG2 cells were maintained in 10 cm culture dishes in DMEM (Gibco) containing 10% calf serum (Hyclone), 1% penicillin/streptomycin (Gibco), and 1% sodium pyruvate (Gibco). HT22 cells (gift from Dr. Stella Tsirka, Stony Brook University) were maintained in DMEM with 10% fetal bovine serum (Atlanta Biologicals) and 1% penicillin/streptomycin. Cells were incubated at 37°C with 5% CO2.

Cells were transfected at 90% confluency with a solution containing serum-free media, GenJet Plus In Vitro Transfection Reagent (2 µls/µg plasmid DNA) (SignaGen Laboratories) and 0.5-2 µg (COS-7, HeLa) or 1-4 µg (N18TG2, HT22) of each plasmid for 3 hours (COS-7, HeLa) or overnight (NT18TG2, HT22). MAGL constructs or empty vector plasmid were co-transfected with GFP, PM-GFP, and pDSRED2-ER constructs at a ratio of 1:2 µg DNA respectively to account for low transfection efficiency of these constructs that occurs during co-transfection. Transfection reagent-containing media was replaced with maintenance media after incubation period.

Cell homogenization and protein quantification

Cells were harvested 24 hours after transfection and mechanically homogenized in 50 mM Tris-HCl (pH 7.4) using a 26-gauge or 30-gauge needle (for neuronal cells). Whole cell lysate was obtained from the soluble fraction after spinning the homogenate at 1,000×*g* for 15 minutes. Protein content was quantified using a BCA Assay Kit (ThermoScientific Pierce).

Western Blot

Five micrograms of transfected cell lysate boiled in SDS-PAGE loading buffer was run on 12% SDS-PAGE for 90 minutes at 110 V. Proteins were then transferred to a nitrocellulose membrane and placed in 5% milk/PBST for 30 minutes at room temperature or overnight at 4°C. Membranes were then probed with 5% milk/PBST containing mouse-anti-myc antibody (1:1000) (Cell Signaling Technologies) and rabbit-anti-calreticulin antibody (1:3000) (ThermoScientific Pierce) for 1 hour at room temperature. Membranes were washed three times with PBST and then placed in 5% milk containing donkey-anti-rabbit and goat-anti-mouse HRP (both 1:10000) for 1 hour at room temperature. Membranes were washed four times with PBST and placed in developing solution for three minutes.

Enzyme activity assay

Reaction mixtures in triplicate containing 50 mM Tris–HCl (pH 7.4), 5 µg transfected cell lysate, 0.5 mg/mL fatty acid free BSA, and JZL184 or vehicle were pre-incubated on ice for 15 minutes. Reaction mixtures were then incubated at 37°C for 15 minutes after addition of [^{3}H]-2-OG(15000 cpm) + 100 nM or 50 µM 2-OG. Two substrate concentrations were used to determine if any differences in activity could be measured at near physiological concentrations (100 nM) or with an excess of substrate (50 µM). Reactions were stopped by the addition of 2 volumes of chloroform:methanol (1:1, *v*/*v*) and spun at 1,000×*g* for 10 min. The aqueous phase was removed for sampling with 3 mL of ScintiVerse (Fisher). Samples were counted using a Beckman LS 6500 scintillation counter. The following controls were used in the experiment: 1) samples with boiled transfected cell lysate plus JZL184 were used as background, 2) samples containing isoform-transfected cell lysate plus JZL184 were used as a measurement of no MAGL activity, and 3) samples with empty vector-transfected cell lysate were used to calculate basal MAGL hydrolytic activity. Average values from control 1, 2, and 3 were subtracted from isoform-transfected cell lysate plus vehicle to obtain final activity values.

Immunofluorescence and imaging

Cells were transferred 24 hours post-transfection to 35 mm dishes containing coverslips. N18TG2 and HT22 were transferred to poly-D-lysine-coated coverslips (50 ug/mL for 1 hour) (Sigma-Aldrich). For the sub-cellular localization experiments, cells were transferred 24 hours later to clean dishes, washed three times with PBS and then fixed with 3% paraformaldehyde for 15 minutes at room temperature. Fixed cells were washed three times with PBS and then permeabilized with 0.2% Triton/0.5% normal goat serum/PBS on ice for 5 minutes. Permeabilization solution was removed and cells were placed in 2% goat serum (GS)/PBS for 30 minutes at room temperature. Blocking solution was removed and coverslips incubated with 5% GS/PBS containing mouse-

anti-myc (1:1500) overnight at 4°C. Samples were then placed in blocking solution for 30 minutes. Coverslips were washed 3 times with 2% GS/PBS for 15 minutes each. Samples were then incubated with either AlexaFluor488 chicken-anti-mouse (1:800) or AlexaFluor594 donkey-anti-mouse (1:800) (Invitrogen) for 1 hour at room temperature. For MAGL construct co-localization experiments, cells were fixed with methanol at-20°C for 10 minutes and then acetone for 30 seconds at the same temperature. Acetone was removed and cells washed three times with PBS at room temperature. Samples were placed in blocking solution for 30 minutes and then incubated with primary antibodies as above. The primary antibodies used were mouse-anti-myc, rabbit-anti-His (1:100) (Cell Signaling Technologies), and mouse anti-FLAG (1:200) (Sigma-Aldrich). Samples were washed with blocking as above and then incubated with AlexaFluor488 chicken anti-mouse and AlexaFluor594 donkey-anti-rabbit (1:800) (Invitrogen) for 1 hour at room temperature. After incubation with secondary antibody, coverslips were washed 3 times with PBS and mounted on microscope slides using Vectashield Hardset Mount (Vector Laboratories).

Cell imaging was performed with a Zeiss LSM 510 Meta NLO two-photon laser scanning confocal microscope using the argon (488 nM) and helium-neon lasers (594 nM). Since only parts of neuronal cells were visible in one plane, all images are composites of scans taken every 1 μM.

Statistical Analysis

Values are expressed as mean±SEM. Statistical significance was evaluated by using GraphPad Prism 4 using one way analysis of variance followed by Tukey's test.

RESULTS

Isolating MAGL and its isoforms from mouse brain cDNA

The presence of the mRNA transcript sequences containing either the putative translation initiation codon at 31 bp or 48 bp upstream of MAGL's start codon was determined by isolating these sequences from whole mouse brain cDNA. These sequences are arbitrarily named MAGL2 (48 bp upstream of MAGL) and MAGL3 (31 bp and will be referred to as such in the rest of this chapter (Fig. 2B). Primers designed against the 5'-ends of the three sequences paired with identical 3'-end primers were used in PCR reactions (see MATERIALS and METHODS for primer sequence details). An approximate 1 kb band was isolated from whole mouse brain cDNA using the primer pair for MAGL. MAGL2 and MAGL3 sequences were also amplified using their respective primer pairs. These sequences were successfully cloned into a pcDNA4-myc/His A vector and used in subsequent experiments (Fig. 3).

MAGL, MAGL2, and MAGL3 expression in mouse brain region and peripheral organ cDNA

The primers that were used to amplify MAGL, MAGL2, and MAG3 in whole mouse brain were also used in PCR reactions using mouse hippocampal and cortical cDNA (Fig. 4). MAGL, MAGL2, and MAGL3 sequences were all present in both the hippocampus and cortex. The presence of the sequences in peripheral organs was also analyzed. To take into account differences in cDNA quality, which can determine the effectiveness of primer annealing, reactions were carried out at multiple annealing temperatures (54.0-60.0°C). This removed false negative from the results. Mouse lung, liver, and kidney cDNA contained all three MAGL sequences (Fig. 5).

Expression of exogenous MAGL, MAGL2, and MAGL3 in non-neuronal and neuronal derived cell lines

MAGL may be post-translationally modified to form MAGL2 or MAGL3. Another possibility is that MAGL2 or MAGL3 may be “pro-proteins” of MAGL and are processed to the smaller protein in the brain. Post-translational modifications or cleavage of proteins can be visualized as a change in molecular weight on a SDS-PAGE. C-terminally myc-tagged MAGL, MAGL2, or MAGL3 were transiently transfected into HeLa (Fig. 6A), COS-7 (Fig. 6B), N18TG2 (mouse neuroblastoma, Fig. 6C), and HT22 (mouse immortalized hippocampal neurons, Fig. 6D) cell lines. Western blot analysis of transfected protein lysates revealed that MAGL-myc is expressed as a protein with a molecular weight of ~37 kDa (protein + tag molecular weight) in both the non-neuronal and neuronal cell types (Fig. 6). A protein present at ~70 kDa seen in seen in HeLa cells (Fig. 6A) indicated that MAGL-myc dimerizes under these conditions. This is not necessarily an indicator of MAGL dimerization *in vivo as* highly hydrophobic proteins such as MAGL tend to dimerize under denaturing conditions. MAGL2-myc is expressed as the largest of the three proteins while MAGL3-myc is expressed as a protein intermediate in molecular weight compared to MAGL-myc and MAGL2-myc in all cell types examined. MAGL2-myc and MAGL3-myc also tend to dimerize under denaturing conditions as indicated by the presence of protein bands twice the size of their corresponding monomers (Fig. 6A & 6C). However, the neuronal MAGL-myc-transfected cell types, as well as the non-neuronal cell types, do not express proteins identical in molecular weight to MAGL2-myc or MAGL3-myc. Neither do the MAGL2-myc nor MAGL3-myc-transfected cells express a protein identical in weight to MAGL-myc.

Enzymatic activity of exogenous MAGL, MAGL2, and MAGL3 in non-neuronal and neuronal cell lines

After confirming the expression of the myc-tagged MAGL isoforms in COS-7, HeLa, N18TG2, and HT22 cell lysates as described above, their enzymatic activities

were measured using a radiometric assay. Five micrograms of transiently transfected cell lysate was incubated with 100 nM or 50 μM 2-oleoylgycerol/[^{3}H]-2-oleoylglycerol at 37°C for 15 minutes. The three MAGL isoforms were active in each cell line examined. The hydrolytic activity of MAGL in HeLa cells with 100 nM substrate was 0.16±0.07 nmol/min/mg (Fig. 7A). The activities of MAGL2 and MAGL3 with 100 nM substrate were 0.11±0.05 nmol/min/mg and 0.08±0.03 nmol/min/mg respectively (Fig. 7A). The activities of the MAGL isoforms incubated with 50 μM substrate in this cell line were 110.5±17.7 nmol/min/mg, 106.7±10.8 nmol/min/mg, and 107.1±22.5 nmol/min/mg for MAGL, MAGL2, and MAGL3 respectively (Fig. 7B). MAGL, MAGL2, and MAGL3 displayed activities of 0.15±0.05 nmol/min/mg, 0.13±0.05 nmol/min/mg, and 0.17±0.04 nmol/min/mg with 100 nM 2-OG/[^{3}H]-2-OG in COS-7 cell lysates respectively (Fig. 7C). Transiently transfected COS-7 cell lysates incubated with 50 μM substrate showed hydrolytic activities of 106.6±16.8 nmol/min/mg for MAGL, 109.8±5 nmol/min/mg for MAGL2, and 108.7±10.5 nmol/min/mg for MAGL3 (Fig. 7D). N18TG2 cell lysate transfected with MAGL and incubated with 100 nM 2-OG/[^{3}H]-2-OG showed an activity of 0.14 ± 0.06 nmol/min/mg (Fig. 6E). N18TG2 cell lysates transfected with MAGL2 and MAGL3 incubated with the same substrate concentration displayed hydrolytic activities of 0.07±0.04 nmol/min/mg and 0.06±0.02 nmol/min/mg respectively (Fig. 7E). Exogenous MAGL, MAGL2, and MAGL3 from N18GT2 cell lysates showed activities of 55.1± 20.4 nmol/min/mg, 73.6±25.6 nmol/min/mg, and 32.7±8.5 nmol/min/mg respectively when incubated with 50 μM substrate (Fig. 7F). Transfected HT22 cell lysates incubated with 100 nM substrate showed hydrolytic activities of 0.11±0.03 nmol/min/mg for MAGL, 0.10±0.02 nmol/min/mg for MAGL2, and 0.14±0.02 nmol/min/mg for MAGL3 (Fig. 7G). Incubations with 50 μM substrate yielded activities of 10.2±2.9 nmol/min/mg for MAGL, 14.9±1.2 nmol/min/mg for MAGL2, and 9.6±1.1 nmol/min/mg for MAGL3 in this cell line (Fig. 7H).

Sub-cellular localization of MAGL, MAGL2, and MAGL3

The sub-cellular localization of MAGL, MAGL2, and MAGL3 was investigated by co-transfecting these constructs with plasmids expressing GFP, plasmid membrane-

localizing GFP, and DSRED that is sequestered to the endoplasmic reticulum (ER). Although GFP is expressed in all parts of a cell (except the plasma membrane), it is used in this study as a cytosolic marker. HeLa and COS-7 co-transfected with any of the MAGL isoform constructs and GFP primarily exhibited uniform co-localization (Fig. 8A & B). This is especially the case with co-transfection of HeLa cells, but some instances of strong perinuclear staining were also detected as seen with co-transfection with GFP and MAGL2-myc. Some transiently transfected COS-7 cells exhibited partial localization with GFP. COS-7 cells co-transfected with MAGL-myc and MAGL3-myc showed distinct perinuclear co-localization with GFP. Co-transfection of GFP with MAGL2-myc showed co-localization in proximity to the plasma membrane. As in the case of non-neuronal cells, N18TG2 showed uniform co-localization with cytosolic GFP, but also strong perinuclear staining as in the case of MAGL-myc and MAGL3-myc co-transfections (Fig. 9A). On the other hand, HT22 cells co-transfected with GFP and MAGL contructs always showed uniform co-localization (Fig. 9B).

Co-transfections of MAGL constructs with PM-GFP in HeLa cells showed a uniform co-localization of MAGL-myc with the plasma membrane, but partial co-localization with MAGL2-myc and MAGL3-myc (Fig.10A). All MAGL constructs showed uniform co-localization with PM-GFP in COS-7 cells (Fig. 10B). Co-localization of PM-GFP with MAGL constructs in neuron-derived cell lines is often partial as in the case of MAGL-myc and MAGL3-myc in N18TG2 and MAGL-myc in HT22 cells (Fig 11A&B). However, uniform co-localization also occurs as was seen with MAGL2-myc in N18TG2 cells and MAGL2-myc and MAGL3-myc in HT22 cells. All MAGL constructs transiently transfected into HeLa, N18TG2, and HT22 exhibited partial co-localization with the ER marker, DSRED-ER as evidenced by the orange-yellow color (Fig. 12A, Fig. 13 A&B). MAGL-myc, MAGL2-myc, and MAGL3-myc displayed uniform co-localization with DSRED-ER in COS-7 cells (Fig. 12B).

Co-localization of MAGL, MAGL2, and MAGL3 in N18TG2 and HT22 cells lines

MAGL constructs with differing C-terminal peptide tags were co-transfected to determine if their co-expression in the presence of neuron-specific proteins altered the

localization patterns seen in the sub-cellular marker co-transfections. As was seen in the sub-cellular localization experiments, MAGL-flag, MAGL2-his, and MAGL3-his co-transfected with empty vector display typical cytosolic staining with both cell types (Fig. 14 A&B columns 1-3). MAGL-flag and MAGL2-his co-transfections showed perinuclear co-localization in N18TG2 and HT22 cells (Fig. 14 A&B column 4). This was also the case in MAGL-flag and MAGL3-his co-transfections (Fig. 14 A&B column 5). Interestingly, these co-transfected proteins also possessed the tendency to form aggregates. Co-transfection of MAGL2-myc and MAGL3-his into N18TG2 and HT22 cells generally showed uniform co-localization throughout the cells (i.e. cell body and branches).

DISCUSSION

MAGL was identified as an enzyme involved in triglyceride metabolism nearly 30 years prior to its identification as the principal enzyme that hydrolyzes the endocannabinoid, 2-AG. As MAGL is a universally expressed protein, one could hypothesize that its regulation of expression and its mechanism of action does not differ between tissues. However, the presence of MAGL isoforms, particularly in the brain, as evidenced by genomic data and western blot analysis, would argue against this idea. Since MAGL is an important modulator of endocannabinoid signaling tone, determining how MAGL expression is regulated and localized to its substrate in neurons would further clarify how 2-AG signaling is terminated in the central nervous system. Expression of isoforms may be part of a specialized mechanism by which 2-AG hydrolysis take place in neurons and perhaps is a way to fine tune this activity. The goal of the present study was to explore this possibility by characterizing expression, enzymatic activity and sub-cellular localization of MAGL isoforms isolated from mouse brain cDNA.

Analysis of mouse whole mouse brain and brain region cDNA revealed that indeed the longest MAGL transcript, transcript variant 1 (MAGL2 and MAGL3), is expressed in the brain and is not specific to either the cortex or hippocampus.

Additionally, transcript variant 1 is also present in the lung, liver, and kidney. This experiment determined that expression of the larger isoforms is not brain-specific. It should be noted that these experiments cannot be used to distinguish MAGL isolated from any particular transcript as the 5'-end primer used to isolate MAGL anneals to sequences shared by all transcript variants. MAGL2 and MAGL3 are also not distinguishable as separate sequences as the only difference between them are the additional 19 base pairs at the 5'-end of MAGL2. It is possible that the successful isolation of MAGL3 resulted from amplification of part of the MAGL2 sequence. However, western blot analysis of exogenous MAGL3 shows that translation can be initiated at its start codon. Another point to consider is that transcript variant 3, a sequence identical to transcript variant 2 except with a 66 bp deletion, should also be amplified with MAGL primers. This 777 bp pair sequence translates into an ~30 kDa protein and may correspond to the protein seen in testes (Karlsson et al., 2001). Absence of a band corresponding to this sequence in mouse brain cDNA, however, confirmed that this isoform is not expressed in the brain and it will not be discussed further.

A recent study examining synthetic mRNA sequences containing two in-frame translation start codons and 5'-UTR of varying lengths determined that translation initiation will favor the upstream start codon with lengthening of the 5'-UTR sequence (Matsuda and Mauro, 2010). The codon favored for translation initiation was also cell-type specific (Matsuda and Mauro, 2010). Using these data, one could hypothesize that transcript variant 1 may be translated at a higher rate than transcript variant 2 in neurons allowing for the expression of the larger isoform in the brain. However, only one band was detected in northern blot analysis of MAGL mRNA in brain and adipose issue (Dinh et al., 2002; Karlsson et al., 2001). A more comprehensive quantitative analysis of brain and other tissue MAGL mRNA would have to be carried out to determine if transcript variant 1 is present at higher levels in the brain than other tissues.

Cloning of these sequences allowed for characterization of MAGL isoform expression, activity, and sub-cellular localization in non-neuronal and neuronal cell types. Western blot analysis of transiently transfected COS-7, HeLa, N18TG2, and

HT22 showed that these isoforms are expressed in non-neuronal and neuronal cell lines. The molecular weights of the MAGL, MAGL2, and MAGL3 matched predicted molecular weights and there was no evidence of gel shift. This would argue against post-translational modification and “pro-protein” cleavage. On the other hand, some post-translational modifications cannot be detected this way. Enzyme activity assays showed that MAGL, MAGL2, and MAGL3 are enzymatically active in COS-7, HeLa, N18TG2, and HT22. There were also no significant differences between the activities of MAGL, MAGL2, and MAGL3 in a particular cell line. This demonstrates that isoform activity is not enhanced by interactions with cell-type specific factors.

As a predicted peripheral membrane protein, MAGL and its isoforms should localize to the cytosolic face of membranes and the cytosol. MAGL, MAGL2, and MAGL3 co-localize with GFP, which is expressed throughout the cell, in both non-neuronal and neuronal cells. Co-localization of MAGL, MAGL2, and MAGL3 with GFP may be variable, however, and co-localization may be seen in close proximity to the plasma membrane only or nucleus only at times. MAGL and its isoforms also co-localize to the plasma membrane, but again, co-localization is variable with complete localization being seen with some cell lines/constructs while partial localization being seen in other instances. MAGL, MAGL2, and MAGL3 also partially localize to the ER in the cell lines examined. This can be attributed to either the high concentration of protein being translated at the ER due to its over-expression or to post-translational modification/cell sorting processes occurring at the ER. It is possible that the amphitrophic nature of MAGL and its isoforms lends to the ambiguous nature of its localization: it may localize to the cytosol, be concentrated at the plasma membrane, or be expressed uniformly. Previous studies have shown both uniform localization of over-expressing MAGL throughout the cytosol as well as strong perinuclear staining (Dinh et al., 2002; Straiker and Mackie, 2009). Overall, the data presented in this study confirms that MAGL and its isoforms localize to the cytosol, ER, and at the plasma membrane.

Co-expression of MAGL with MAGL2 or MAGL3 in N18TG2 and HT22 cells determined that these constructs co-localize and tend to form aggregates. Again, this may be a consequence of an increase of protein translation occurring due to over-expression of the isoforms and not as a result of some cellular function *per se*.

Generally, aggregating proteins are targeted for degradation, but previous studies have also shown that aggregates are sites of sequestration for other proteins in the cell (Snapp et al., 2003; Cheng et al., 2007).

CONCLUSIONS and FUTURE DIRECTIONS

The present study sought to discover the origin of the ~35 kDa form of MAGL expressed in the brain by isolating predicted isoforms from whole mouse brain cDNA. These isoforms would offer an explanation for the expression of the larger MAGL isoform as they are ~1-2 kDa larger than MAGL. Experiments confirmed the presence of transcript variant 1 of MAGL in brain and in peripheral organs. Characterization of MAGL and its longer isoforms, however, showed that these proteins overlap in their function. They display similar enzymatic activities, can all be expressed in both non-neuronal and neuronal cell lines, and localize to the cytosol, plasma membrane, and ER.

Translation of transcript variant 1, the transcript from which MAGL2 or MAGL3 is translated, may occur at higher rate in neurons than other cell types. A more comprehensive Northern blot analysis of MAGL mRNA in brain, adipose, and other tissues would help clarify if indeed MAGL mRNA is universally expressed as only one band. Quantitative RT-PCR of transcript variant 1 and 2 would also clarify if either is transcribed at a higher rate in the brain relative to other peripheral tissues. Post-translational modifications of any of these isoforms are also still a possibility as not all modifications can be detected by SDS-PAGE. Further analyses of post-translational modifications could be carried out by using post-translational modification prediction programs and testing for predicted modifications using available assays. For example, phosphorylation of proteins can be tested for by using phosphorylation inhibition assays. Additionally, using native-PAGE may also reveal interactions of MAGL or any of its isoforms with neuron-specific proteins that are disrupted in SDS-PAGE. The redundancy in MAGL isoform activity could change upon modulation of the intracellular environment via incubation with 2-AG or stimulating endogenous 2-AG production.

There are other protein isoforms that are differentially activated. For example, protein kinase C isoform function is regulated via different mechanisms. Isoforms of this kinase are not only expressed in a tissue-specific manner, but are also stimulated to change their sub-cellular localization by different factors (Steinberg, 2008). Incubations with 2-AG or stimulating endogenous 2-AG production may induce tissue-specific changes in MAGL transcription/translation and/or stimulate protein interactions necessary for the expression of the ~35 kDA isoform of MAGL. Ultimately, purification of the larger MAGL isoform in the brain will determine the structural properties (i.e. peptide sequence and/or post-translational modifications) that distinguish it from its lower molecular weight counterpart. Total redundancy in function of these isoforms is unlikely since expression of the ~35 kDa isoform is tissue-specific. Additionally, endogenous 2-AG levels are significantly higher than other MAGs in the brain as compared to peripheral tissues following inhibition of MAGL (Long et al., 2009). This offers another argument against total functional overlap of these MAGL isoforms. The study presented here is significant because it provides the first evidence that mouse MAGL transcript 1 mRNA is present in the brain and other organs and that proteins translated from this transcript, MAGL2 and MAGL3, possess characteristics similar to MAGL.

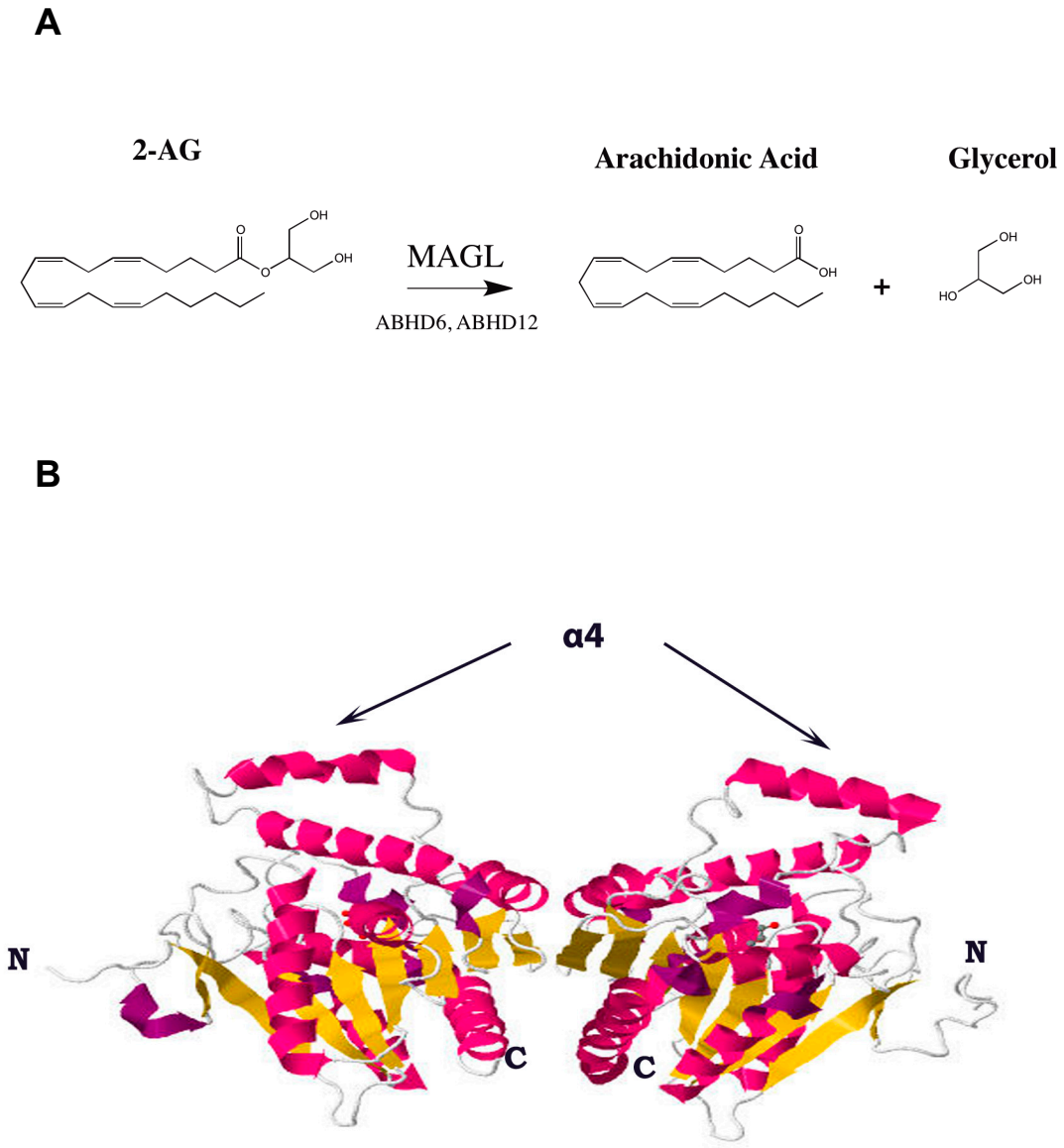

Figure 1. 2-AG hydrolysis (A) and crystal structure of human MAGL (B). A) 2-AG is hydrolyzed principally by MAGL as well as ABHD6 and ABHD12 to arachidonic acid and glycerol. **B)** Human MAGL (303 aa, transcript variant 2) represented as a dimer in closed conformation. Interaction of the amphitrophic helix, α4, with the membrane is thought to induce conformational change in the enzyme to expose the active site to its substrate. N- and C-termini of the enzyme monomers are also labeled. *Image from RCSB Protein Database (www.pdb.org) of PDB ID 3HJU (Labar et al., 2010).*

A

```
transcript variant 1     cccaaacagacttgtgcccgtcaactgcatcttcccagaccggtgtgggaacaacggccaggtccacgtcctgtgtggcg   80
transcript variant 2     ---------------------------------------------------------------------------------

transcript variant 1     tgccgatgacagccgcgaggtttccttccctaagcggtcgcgggcgggcaagaggcaaagtttgtcggagaatcggggtg   160
transcript variant 2     ---------------------------------------------------------------------------------

transcript variant 1     actttgctcggggacccgcatctgcgcgaatgcgcggtgccgcggagcgcgtctcgcagcagctccgggctggggaccgg   240
transcript variant 2     ---------------------------------------------------------------------------------

transcript variant 1     ctgtccctcgctcccggaacccctcaggggtgtgttctggaaaagtggcgacatgagctagagctggagcagcaggagg   320
transcript variant 2     ------------------------------------------------------------------------gggccg   6

transcript variant 1     gagcaactcgcacccctgcagcccaggcggggagggcgcggaccccgtggtgctgccctgcggccgcgatgagggaacag   400
transcript variant 2     ccccgccgccgagcggctggggataaagtggcggcgcagacgccgcgccctatcgctgcgcagccggccgcgcgcagta   86
                                                                                                  ↓
transcript variant 1     ccctcgtttgcctggcgctgatactcgaggctgtggcggtagtggaATGcaaaagccaagactaATGgaaacagggccta   480
transcript variant 2     gtctggctctagcccgccgcagacccggacccgcgtggtgctcggggaacgtgacagcggcgctcgtggcccggggccta   166

transcript variant 1     aagacccctgcaggATGcctgaggcaagttcacccaggcgaactccacagaatgttccctaccaggacctgcctcacctg   480
transcript variant 2     aagacccctgcaggATGcctgaggcaagttcacccaggcgaactccacagaatgttccctaccaggacctgcctcacctg   246

transcript variant 1     gtcaatgcagacggacagtacctcttttgtagatactggaagcccagtggcacacccaa                       539
transcipt  variant 2     gtcaatgcagacggacagtacctcttttgtagatactggaagcccagtggcacacccaa                       305
```

B

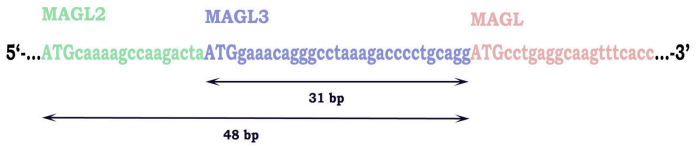

Figure 2. 5'-UTR, exon 1, and exon 2 of MAGL Transcript Variant 1 and 2. A) 5' UTR of Transcript variant 1 and 2 with in-frame translation initiation start codons shown in capital letters. The arrow indicates the exon1-exon2 splice site. Note the sequences are identical starting from the exon1-exon2 splice site. Transcript variant 3 shares an identical 5'-UTR with transcript variant 1 and therefore is not pictured (see text for details). **B)** 5'-end primer sequences of MAGL (pink), MAGL2 (green), and MAGL3 (blue) as designed by the sequence in **A.**

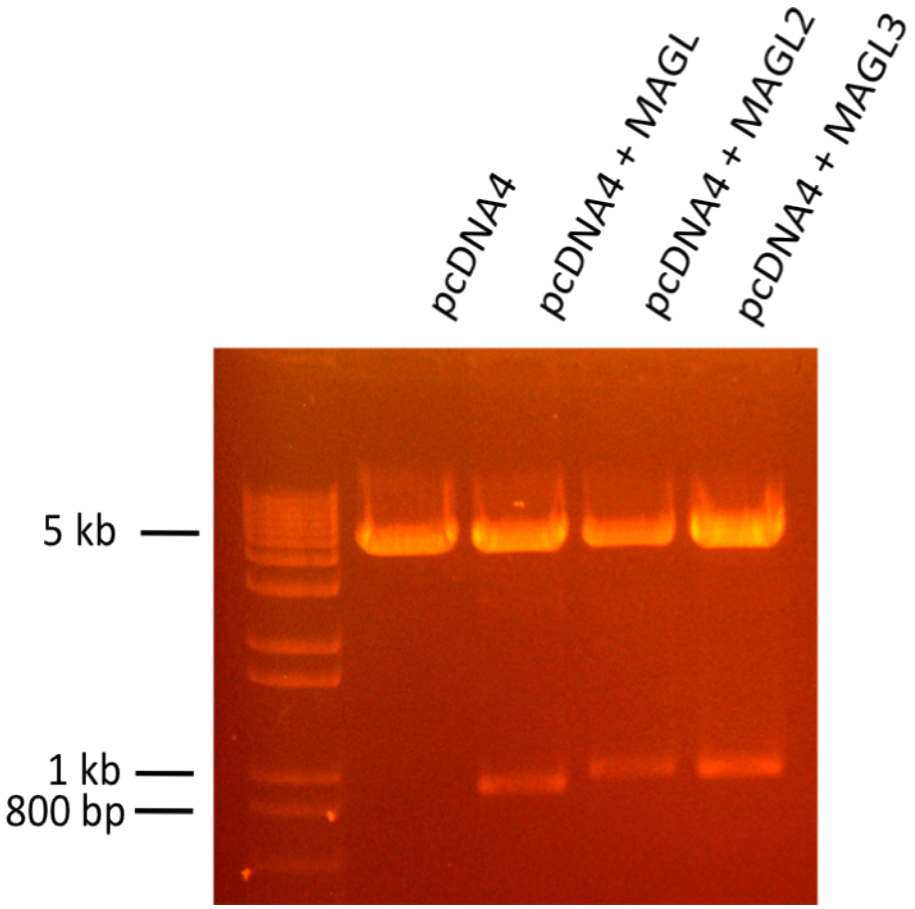

Figure 3. Restriction Digest of MAGL isoform constructs. MAGL isoform constructs were digested with *KpnI*/*XhoI* to confirm insertion into the vector after isolation from mouse brain cDNA.

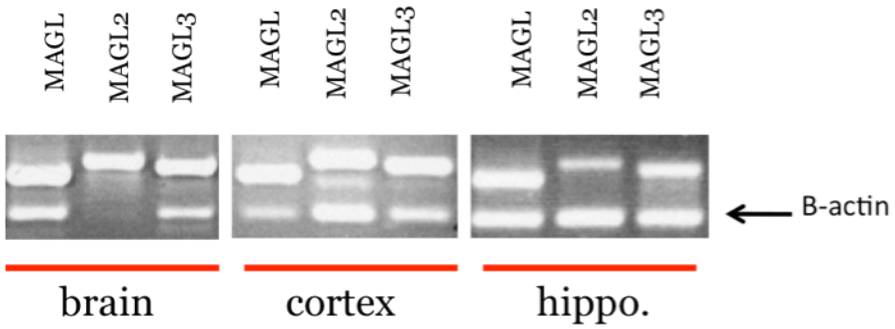

Figure 4. MAGL, MAGL2, and MAGL3 cDNA in mouse brain regions. Coritcal and hippocampal cDNA were used in PCR reactions utilizing the 5'-end primers used to clone MAGL, MAGL2, and MAGL3 and an identical 3'-end primer. Primers for β-actin were used as an internal control.

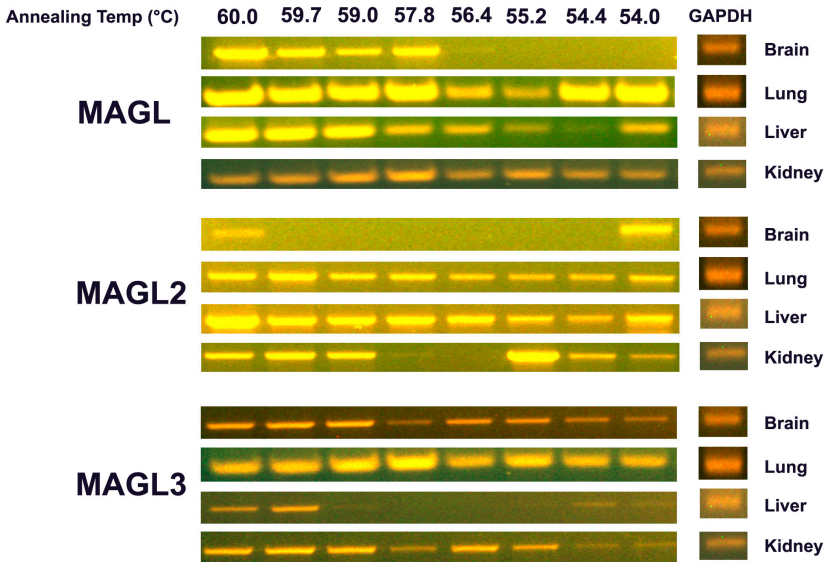

Figure 5. MAGL, MAGL2, and MAGL3 cDNA in brain and peripheral organs. Whole mouse brain, lung, liver, and kidney cDNA were used in PCR reactions utilizing the 5'end primers used to clone MAGL, MAGL2, and MAGL3 and an identical 3'-end primer. Reactions were carried out with an annealing temperature gradient to account for differences in cDNA quality and ensure absence of false negatives. Primers for GAPDH were used as an internal control.

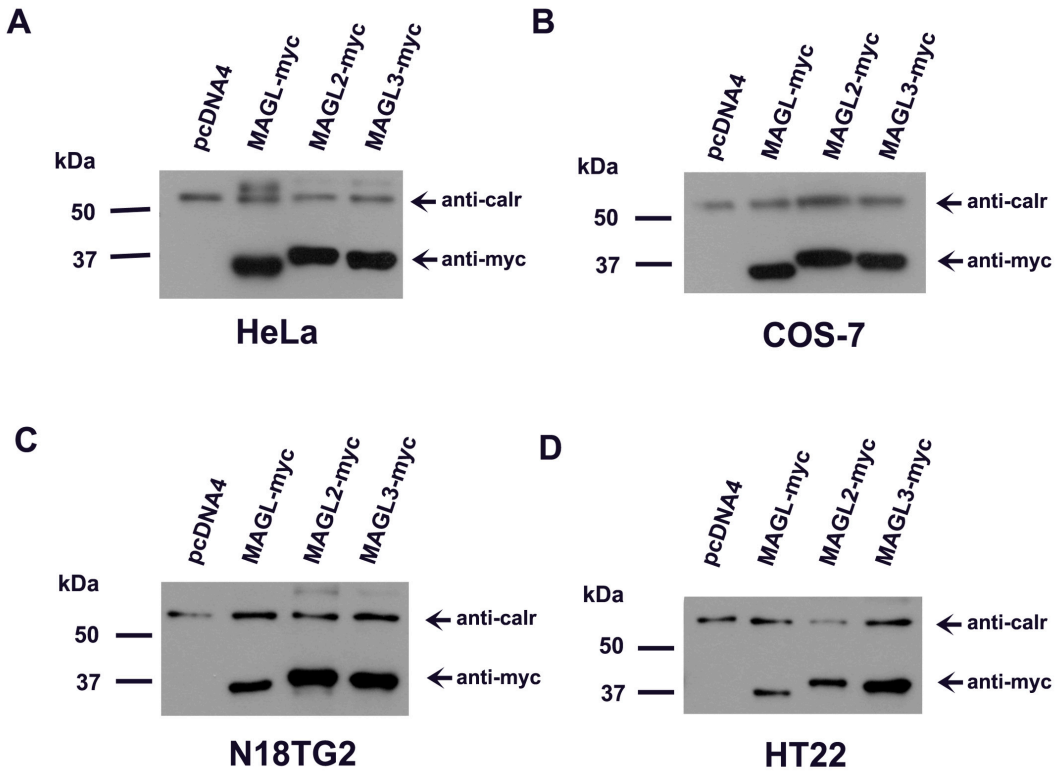

Figure 6. Western blot analysis of cells expressing exongenous MAGL, MAGL2, and MAGL3. Five micrograms cell lysate from transiently transfected HeLa (A), COS-7 (B), N18TG2 (C), and HT22 (D) cells expressing myc-tagged MAGL, MAGL2, and MAGL3 at their expected molecular weights. Calreticulin is used as a control.

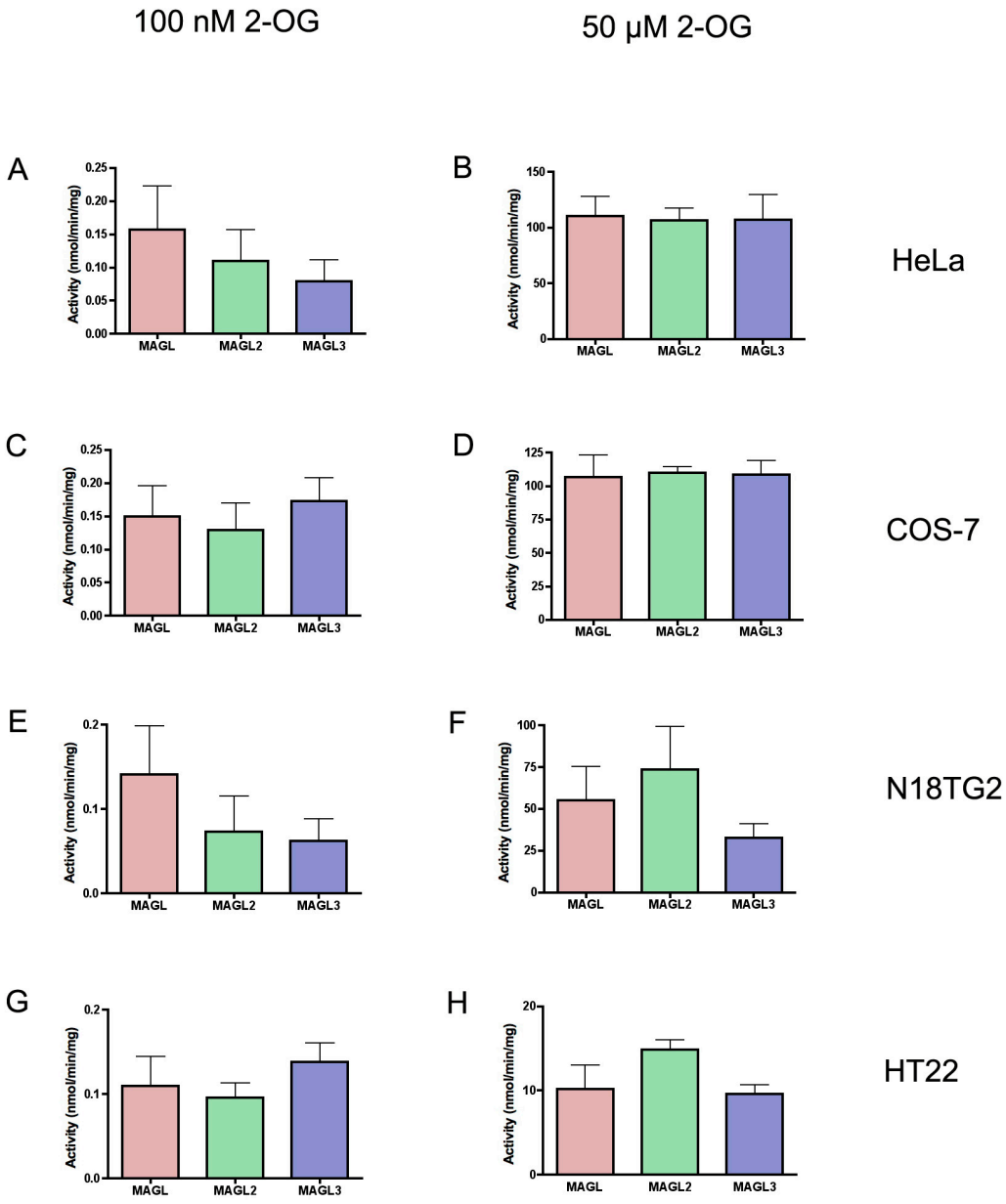

Figure 7. Enzymatic Activity of MAGL, MAGL2, and MAGL3 in non-neuronal and neuronal cells lines. Five micrograms cell protein lysate of transiently transfected HeLa, COS-7, N18TG2, and HT22 cells were incubated with either 100 nM (A, C, E, G) or 50 µM 2-OG/^{3}H-2-OG (15000 cpm) (B, D, F, H) for 15 minutes at 37°C. Activities are expressed as mean±SEM (n=3). There were no significant differences in enzyme activities as evaluated by One way-ANOVA followed by Tukey's test.

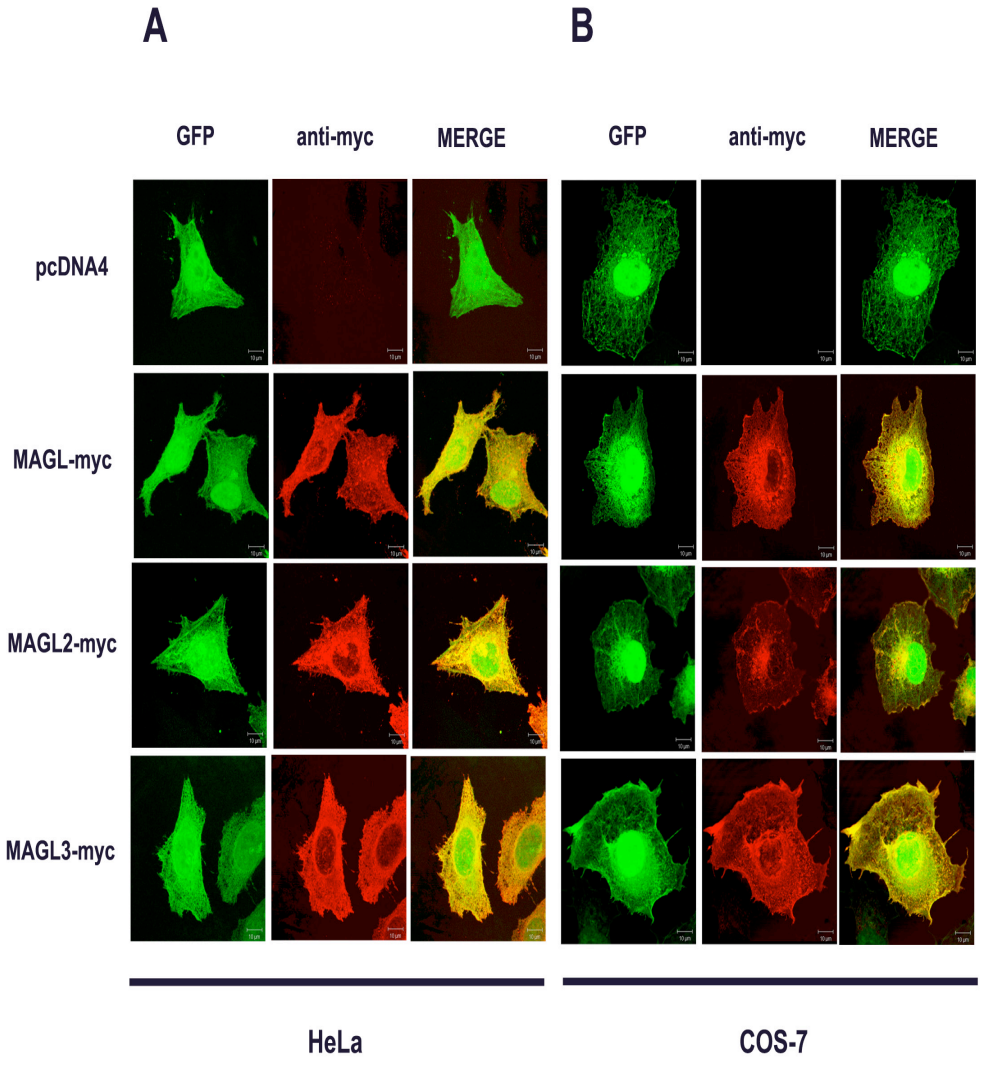

Figure 8. Co-localization of MAGL, MAGL2, and MAGL3 with GFP in non-neuronal cells. Co-localization in HeLa **(A)** and COS-7 **(B)** transiently co-transfected with myc-tagged MAGL, MAGL2, and MAGL3 and GFP is shown. GFP is shown in green, myc-tagged protein in red, and merge in yellow. Images are composites of pictures taken every 1 μM through the cell.

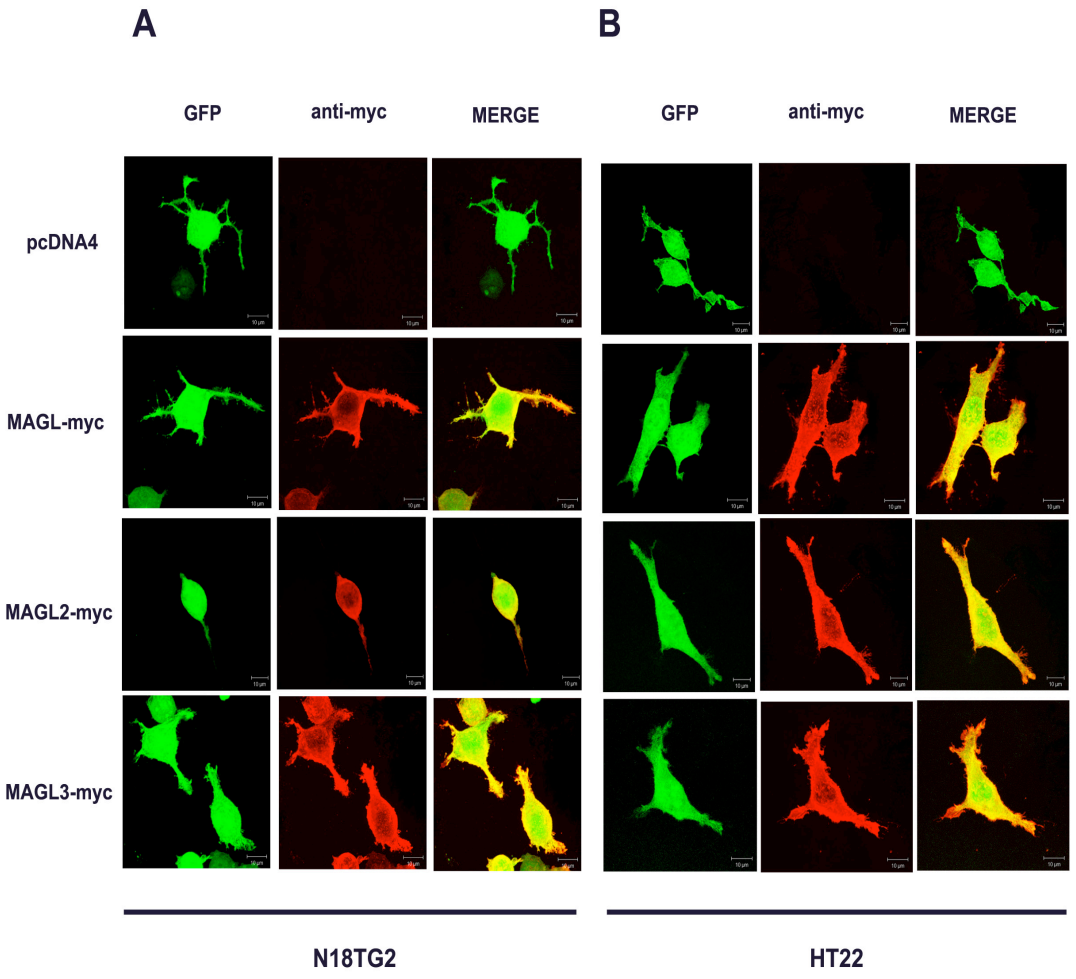

Figure 9. Co-localization of MAGL, MAGL2, and MAGL3 with GFP in neuronal cells. Co-localization in N18TG2 **(A)** and HT22 **(B)** transiently co-transfected with myc-tagged MAGL, MAGL2, and MAGL3 and GFP is shown. GFP is shown in green, myc-tagged protein in red, and merge in yellow. Images are composites of pictures taken every 1 μM through the cell.

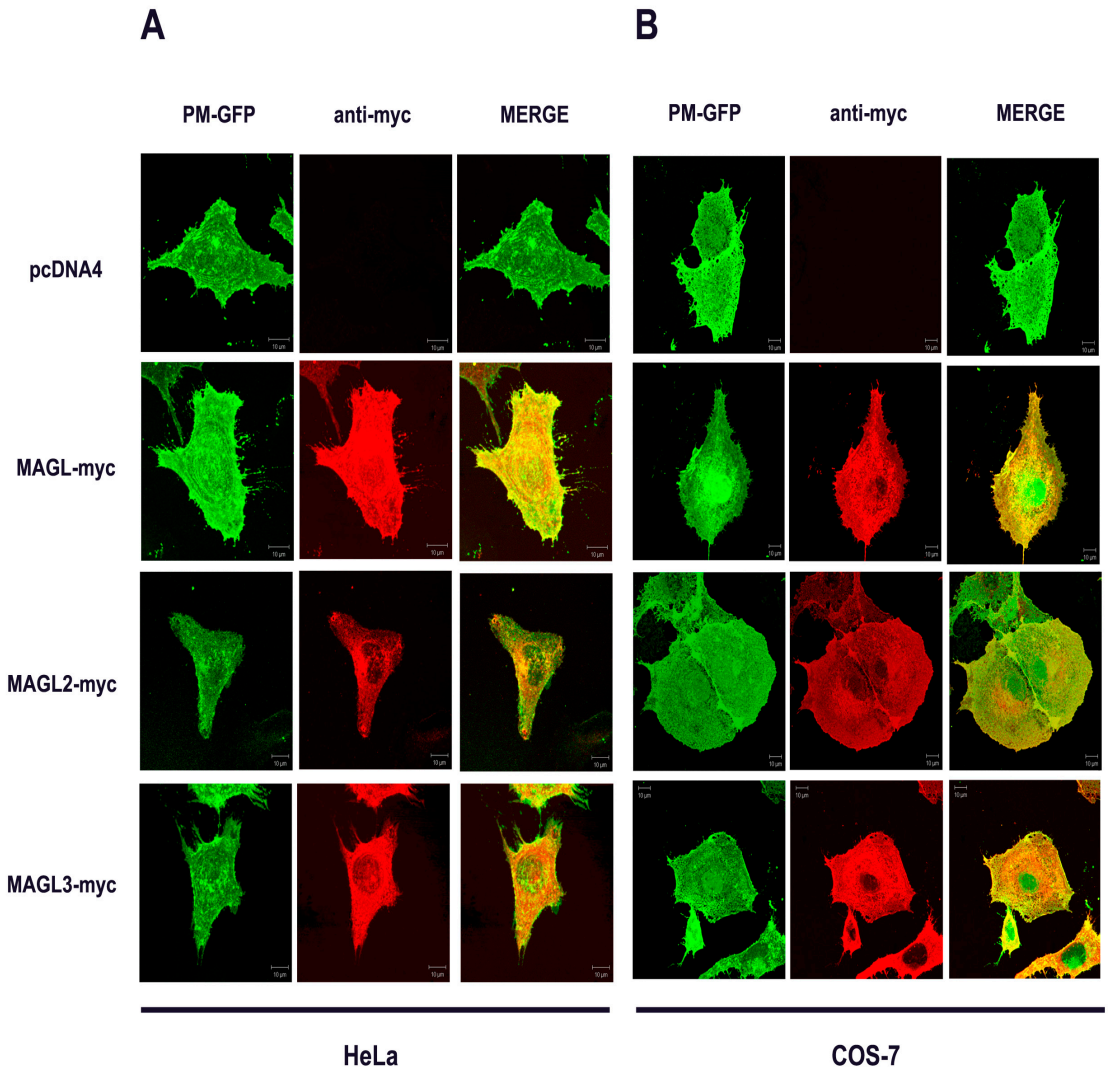

Figure 10. Co-localization of MAGL, MAGL2, and MAGL3 with PM-GFP in non-neuronal cells. Co-localization in HeLa **(A)** and COS-7 **(B)** transiently co-transfected with myc-tagged MAGL, MAGL2, and MAGL3 and PM-GFP is shown. PM-GFP is shown in green, myc-tagged protein in red, and merge in yellow. Images are composites of pictures taken every 1 μM through the cell.

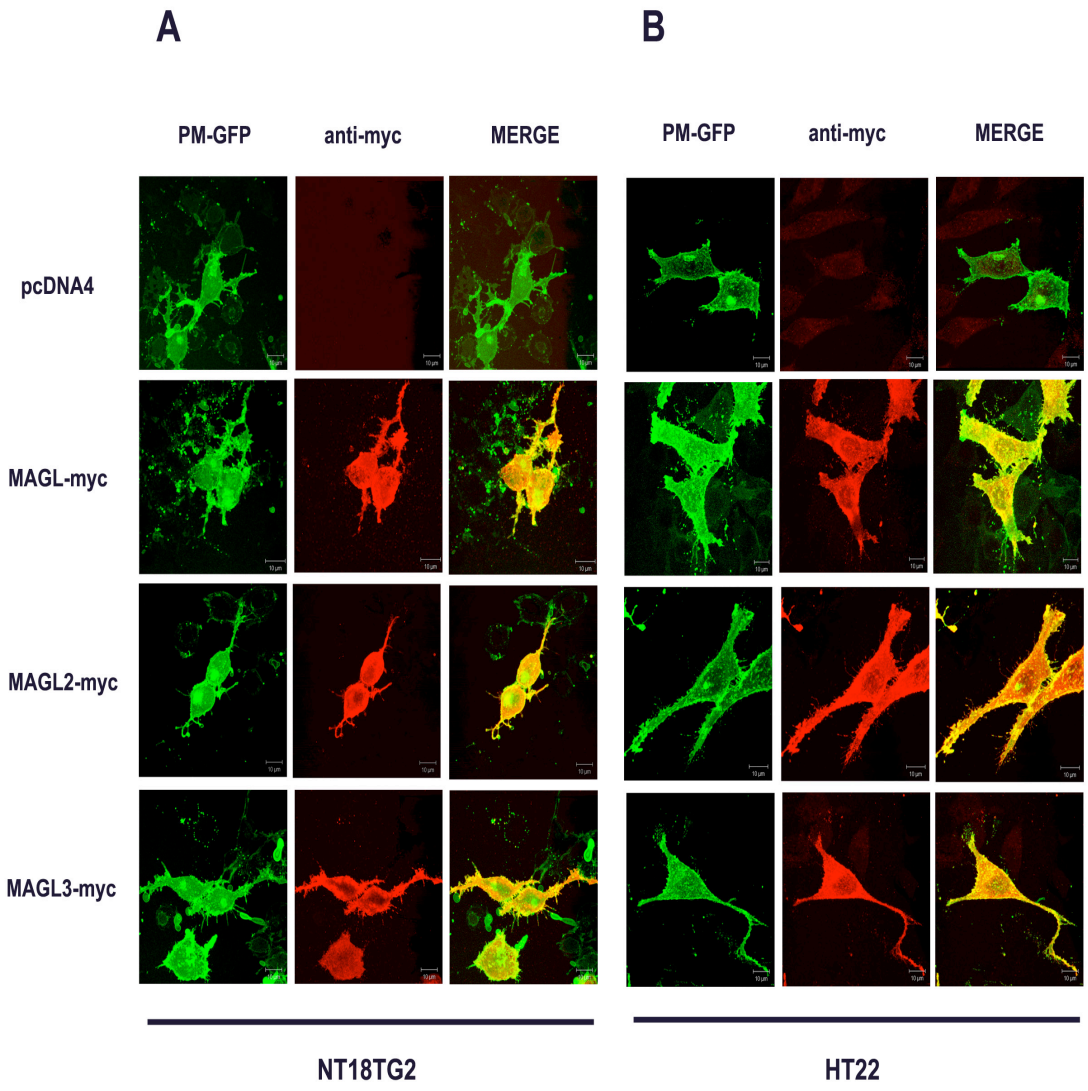

Figure 11. Co-localization of MAGL, MAGL2, and MAGL3 with PM-GFP in neuronal cells. Co-localization in N18TG2 **(A)** and HT22 **(B)** transiently co-transfected with myc-tagged MAGL, MAGL2, and MAGL3 and PM-GFP is shown. GFP is shown in green, myc-tagged protein in red, and merge in yellow. Images are composites of pictures taken every 1 μM through the cell.

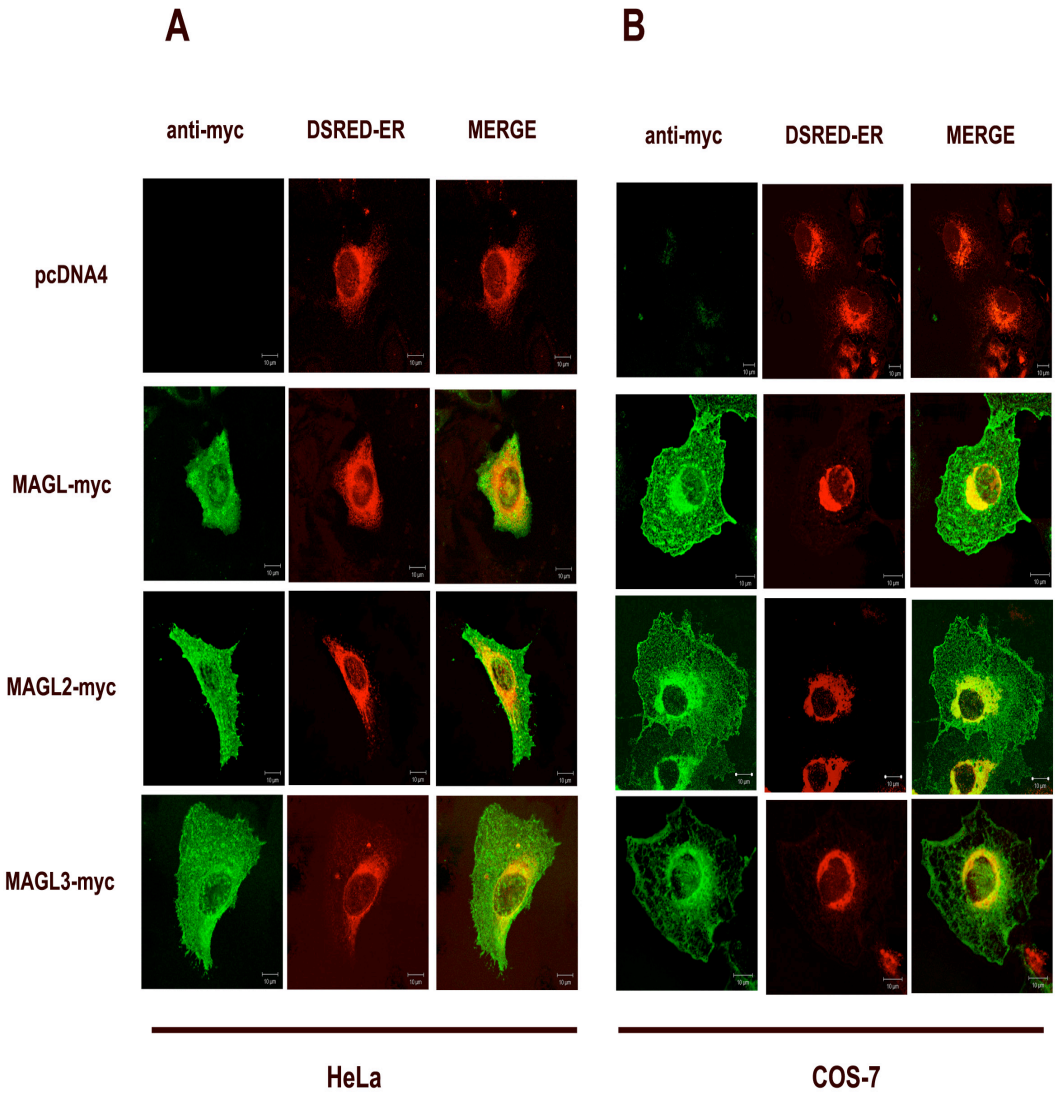

Figure 12. Co-localization of MAGL, MAGL2, and MAGL3 with DSRED-ER in non-neuronal cells. Co-localization in HeLa **(A)** and COS-7 **(B)** transiently co-transfected with myc-tagged MAGL, MAGL2, and MAGL3 and DSRED-ER is shown. DSRED-ER is shown in red, myc-tagged protein in green, and merge in yellow. Images are composites of pictures taken every 1 μM through the cell.

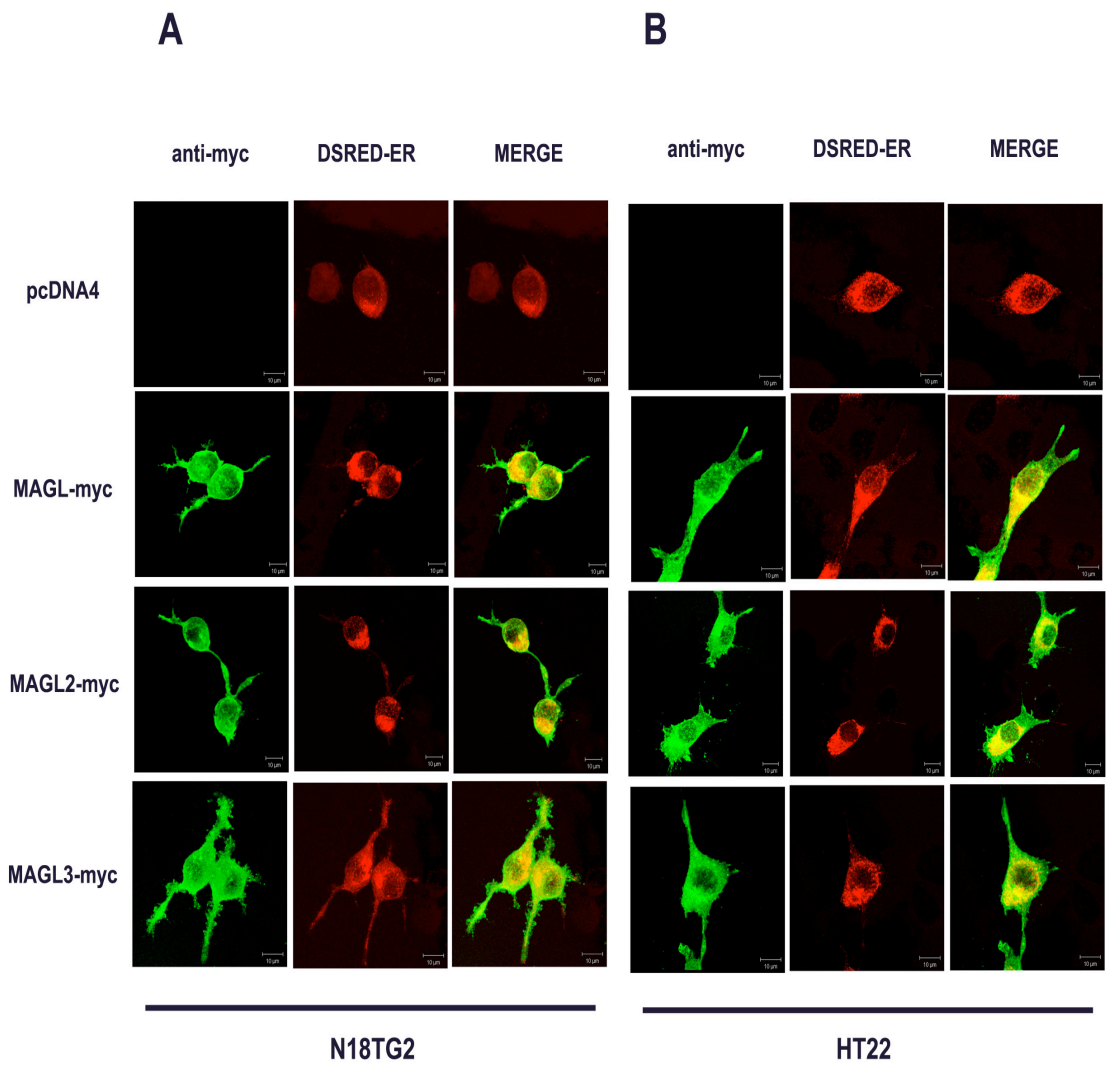

Figure 13. Co-localization of MAGL, MAGL2, and MAGL3 with DSRED-ER in neuronal cells. Co-localization in N18TG2 **(A)** and HT22 **(B)** transiently co-transfected with myc-tagged MAGL, MAGL2, and MAGL3 and DSRED-ER is shown. DSRED-ER is shown in red, myc-tagged protein in green, and merge in yellow. Images are composites of pictures taken every 1 μM through the cell.

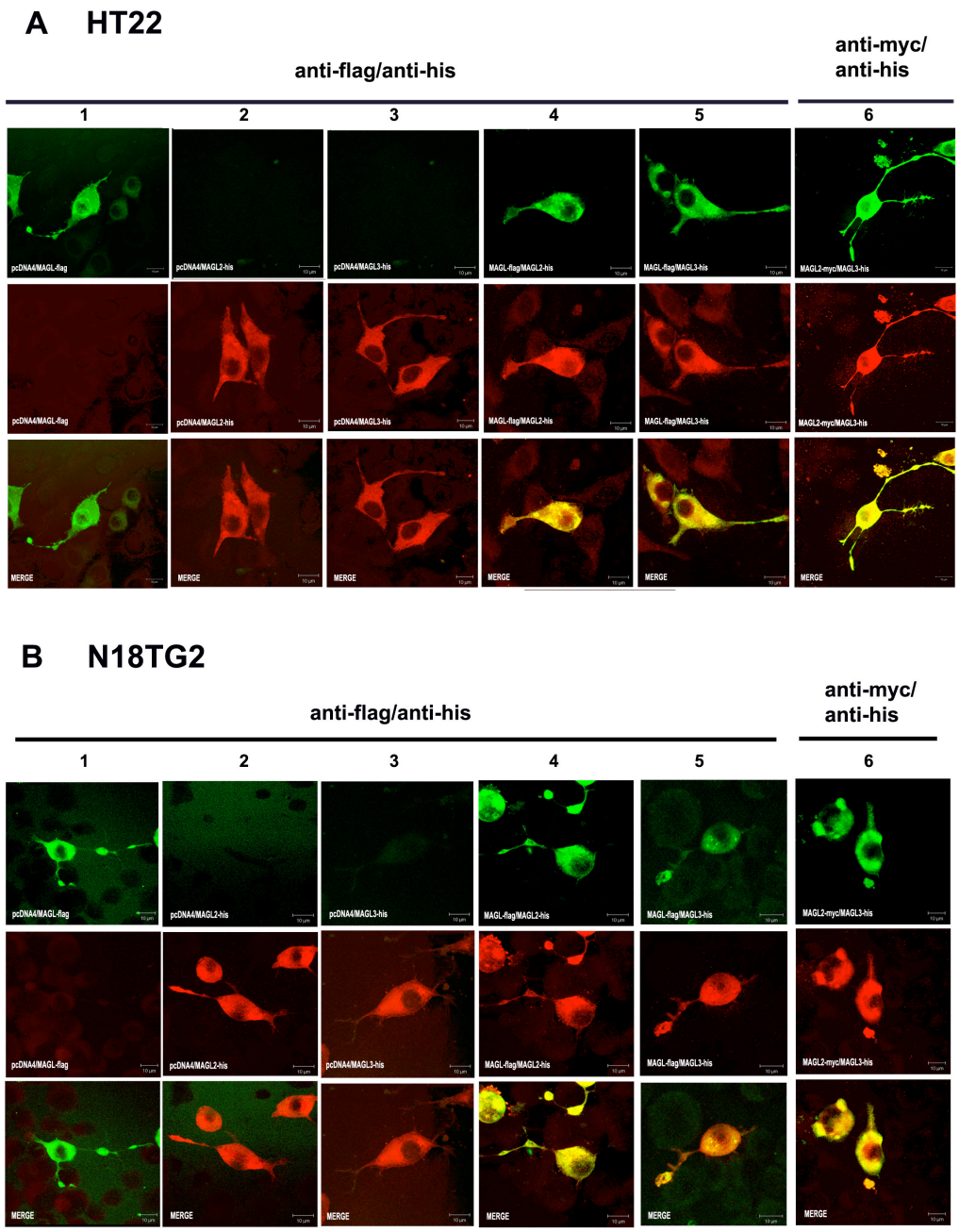

Figure 14. Co-localization of MAGL, MAGL2, and MAGL3 in neuronal cells. N18TG2 **(A)** and HT22 **(B)** transiently co-transfected with empty vector and MAGL-flag, MAGL2-his, or MAGL3-his (columns 1-3), MAGL-flag and MAGL2-his (column 4), MAGL-flag and MAGL3-his (column 5), MAGL2-myc and MAGL3-his (column 6) is shown. Flag-tagged protein is shown in green, his-tagged protein in red, and myc-tagged protein in green. Merged images are the bottom row of both **(A)** and **(B)**. Images are composites of pictures taken every 1 µM through the cell.

Chapter 3

Assessment of a Spectrophotometric Assay for Monoacylglycerol Lipase Activity

ABSTRACT

The endocannabinoid, 2-arachidonoylglycerol (2-AG) is known to play a role in various physiological functions. Monoacylglycerol lipase (Ludanyi et al.), a serine hydrolase, is the principal enzyme responsible for the hydrolysis of 2-AG. MAGL activity is usually measured by costly radiometric or time-consuming mass spectrometric assays. An assessment of a spectrophotometric assay was carried out to determine its usefulness as an alternative method. MAGL obtained from transiently transfected COS-7 cells was incubated with arachidonoyl-1-thio-glycerol, a thioester-containing analog of 2-AG. The thioglycerol that is reacted with 5,5'-dithiobis(2-dinitrobenzoic acid) results in the release of a thiolate ion that has measurable absorbance at 412 nm. This spectrophotometric assay was used to measure MAGL kinetics, activity in sub-cellular fractions and a catalytically inactive mutant, and measure inhibition by the sulfhydryl inhibitor, *N*-arachidonyl maleimide (NAM). Although the spectrophotometric assay could not detect inhibition of MAGL at the lowest concentrations of NAM, most results obtained were comparable to those reported in previous studies. The spectrophotometric assay, therefore, is a useful tool for general purposes such as initial high-throughput screening of inhibitors.

INTRODUCTION

2-AG hydrolysis may be quantified by mass spectrometry or assays with radioactive substrate. Mass spectrometry is impractical for high-throughput assays, while radioactively labeled 2-AG is very costly. Radio-labeled 2-oleoylglycerol (2-OG),

which does not bind to cannabinoid receptors, is often used as a substitute for 2-AG since MAGL hydrolyzes both at similar rates (Chau and Tai, 1988; Saario and Laitinen, 2007). Nevertheless, radioactive 2-OG is still relatively expensive. In this study we explored an alternative method of measuring 2-AG hydrolysis based upon reagents originally developed by Cayman Chemical Company to measure the potency of MAGL inhibitors. The assay employs a thioester-containing analog of 2-AG, arachidonoyl-1-thio-glycerol (A-1-TG), which MAGL can hydrolyze. The thioglycerol released upon hydrolysis by MAGL reacts with 5,5'-dithiobis(2-dinitrobenzoic acid) (DTNB) resulting in the release of a yellow thiolate ion (TNB) (Fig. 15) (Riddles et al., 1983). This assay was utilized to measure MAGL kinetics, activity in cytosolic and membrane fractions, and loss of activity in a catalytically inactive mutant. Saario et al. developed the inhibitor *N*-arachidonyl maleimide (NAM) that irreversibly binds to sulfhydryl groups of cysteine residues (Cys208 and Cys242) in the active site of MAGL (King et al., 2009; Saario et al., 2005; Zvonok et al., 2008). The potency of this inhibitor was measured using the spectrophotometric assay and a conventional radioactive assay using ^{3}H-2-OG for comparison. These experiments serve to measure the assay's applicability and limitations.

MATERIALS and METHODS

Materials

N-arachidonyl maleimide, methylarachidonyl fluorophosphonate, and arachidonoyl-1-thio-glycerol were purchased from Cayman Chemical Company (Ann Arbor, MI, USA). 5,5'-dithiobis(2-dinitrobenzoic acid) and 2-oleoylglycerol were purchased from Sigma-Aldrich (St. Louis, MO, USA). Mono-oleoyl glycerol racemic 2-[glycerol-1 2 3-3H] (1mCi/mL) was purchased from American Radiolabeled Chemicals (St. Louis, MO, USA).

MAGL Cloning and Mutagenesis

Total mRNA was extracted from mouse brain using the RNAeasy Mini Kit(Qiagen RNA). Mouse MAGL cDNA was generated from whole mouse brain mRNA using SuperScriptIII First-Strand Synthesis for RT-PCR (Invitrogen) and cloned into a pCDNA4/TO/myc-HISA vector (Invitrogen). The Ser122Ala mutation was obtained using the PCR Overlap Extension Method as described by Heckman and Pease (Heckman and Pease, 2007). Dual PCR reactions containing 1) a forward primer annealing to **the** 5' end of MAGL (5'-GATATAGGTACCGCCACCATGCCTGAGGCAAGTTCACC-3') and a reverse mutation primer (5'-GAAGGAGGACCCGGTG**C**GGTACCCGCCACGGT-3') and 2) a forward mutation primer (5'-TTCCTCCTGGGCCAC**G**CCATGGGCGGTGCCATC-3') and a reverse primer annealing to the 3' end of MAGL (5'-GATATATCTCGAGTCAGGGTGGACACCCAGC-3') initially inserted nucleotide changes into fragments of the MAGL sequence. Amplification products from both of these reactions were used as templates for a second PCR reaction using MAGL 5'- and 3'-end primers. PCR reactions were carried out using Platinum Pfx DNA Polymerase (Invitrogen) using the following cycling conditions: denaturing at 95°C for 30 seconds, annealing for 1 minute, and elongation at 68°C for 30–60 seconds (35 cycles). The amplification product from this reaction was gel extracted using QIAquick Gel Extraction Kit (Qiagen), subjected to restriction digest with *KpnI* and *XhoI* (New England Biolabs), and re-ligated to the pCDNA4 vector. The vector with insert was grown in competent DH5α *E. coli* (Invitrogen) and isolated using the QIAPrep Spin Miniprep Kit (Qiagen). Insertion of mutated nucleotides was confirmed by Big Dye Terminator Sequencing (Applied Biosystems, Stony Brook HSC Sequencing Facility) over the entire open reading frame. The nucleotides in bold are nucleotide changes while underlined nucleotides are restriction enzyme recognition sites in the above oligomer sequences.

Tissue Culture and Transfection

COS-7 cells were maintained in 10cm culture dishes in DMEM (Gibco) containing 10% Calf Serum (Gibco), 5% Penicillin/Streptomycin (Gibco), and 5% Sodium Pyruvate (Gibco). Cells were transfected at ~70% confluence using 6 μg cDNA with Lipofectamine 2000 (Invitrogen) as prescribed by manufacturer.

Cell Homogenization and Protein Quantification

Cells were harvested 24 hours after transfection and mechanically homogenized in 20mM Tris/1 mM EDTA pH 8.0 (with 320 mM sucrose for fractionation) using a 26-gauge needle. Whole cell lysate was obtained from the soluble fraction after spinning the homogenate at 1000x*g* for 15 minutes. Membrane and cystosolic fractions were obtained by spinning whole cell lysate at 100,000x*g* for 30 minutes. Protein content was quantified using the Pierce BCA Assay Kit.

Spectrophotometric Assay

Reaction mixtures containing 10 mM Tris/1 mM EDTA pH 7.2, MAGL-transfected lysate, membrane, or cytosolic fraction, and inhibitor or vehicle were pre-incubated at 4°C (or room temperature for NAM) for 15 minutes. They were then incubated at 37°C for 3-5 minutes after addition of A-1-TG. One millimolar DTNB was added to the reactions at room temperature. Absorbances were read at 412 nm in 1 cm cuvettes using a Pharmacia Biotech Ultraspec 2000. A cuvette containing only buffer was used as a blank. The concentration of thiolate ion per reaction was calculated using the Beer-Lambert equation, $A=\varepsilon c l$, where A is the absorbance, ε is the molar extinction coefficient (14,150 $M^{-1}cm^{-1}$), c is the concentration, and *l* is the path length. The thiolate concentration is proportional to the thioglycerol concentration and thus a measure of substrate hydrolysis efficiency.

Radiometric Assay

Reaction mixtures containing 10 mM Tris-HCl (pH 8.0), MAGL-transfected lysate, 0.5 mg/mL fatty acid free BSA, and NAM or vehicle were pre-incubated at room temperature for 15 minutes. They were then incubated at 37°C for 15 minutes after addition of 0.8 nCi [^{3}H]-2-OG + 70 µM 2-OG. Reactions were stopped by the addition of 2 volumes chloroform:methanol (1:1, v/v) and spun at 1000x*g* for 10 minutes. The aqueous phase was removed for sampling with 3 mL of ScintiVerse (Fisher). Samples were counted using a Beckman LS 6500 scintillation counter.

Data Analyses

Goodness of fit, kinetic constants, and statistical significance were determined by using GraphPad Prism 4. Statistical significance was evaluated by using two-tailed unpaired *t* tests.

RESULTS

Measuring MAGL kinetics, cytosolic and membrane fraction activity, and loss of activity in a catalytically inactive mutant

Experiments were conducted to determine if results obtained with the spectrophotometric assay were comparable to those obtained in previous radiometric studies. Increasing amounts of MAGL-transfected COS-7 cell lysate were incubated with 200 µM A-1-TG. MAGL activity increased linearly with up to 11 µg cell lysate protein (R^2 = 0.96, Fig. 16A). An apparent K_m= 67.9 ± 3.0 µM and V_{max}= 659.5 ± 81.8 nmol/min/mg were obtained when increasing amounts of A-1-TG were incubated with 5 µg MAGL-transfected cell lysate protein (Fig. 16B). A comparison of MAGL activity in

membrane versus cytosolic fractions revealed contributions of 49.2±2.**0**% and 50.8±2.**0**% to total activity, respectively (Fig. 17A). Mutation of catalytic serine 122 to an alanine (MAGLS122A) abolished hydrolytic activity in both membrane and cytosolic fractions (Fig. 17B).

Quantification of the inhibition of MAGL activity by NAM using spectrophotometric and radiometric assays

In this set of experiments the rates of hydrolysis of the substrates for the spectrophotometric and radiometric assays were 605.3 and 74.2 nmoles/min/mg protein (n=6) with 3.2% and 5.8% relative standard errors of the mean, respectively. The spectrophotometric assay was also compared to the radiometric assay to test its sensitivity. Shown in Figure 18 is a typical experiment where the effects of increasing amounts of the inhibitor NAM on MAGL activity was measured using both assays. An IC_{50} of 45.7 nM and 94.3 nM was obtained for the radiometric and spectrophotometric assay respectively. At the lowest NAM concentration (10^{-9} M) the spectrophotometric assay was not sensitive enough to detect inhibition. The spectrophotometric assay and the radiometric assay between 10^{-8} M NAM, to 10^{-6} M NAM were comparable. Very high concentrations of NAM (10^{-6} and 10^{-5} M) gave nearly complete inhibition of MAGL activity for both assays.

DISCUSSION

The study of 2-AG metabolism is crucial to understanding its physiological function as its synthesis and hydrolysis are tightly coupled to cannabinoid receptor activation. MAGL, as the major enzyme for 2-AG hydrolysis, is an attractive target for inhibitor design. Although cloned more than a decade ago, few selective inhibitors for MAGL have been synthesized. This may be owing to, in part, the lack of available fast,

cost-effective assays. The experiments performed in this study used a spectrophotometric assay to look at MAGL hydrolytic activity and the effect of an inhibitor upon the enzyme.

The proportional increase of MAGL activity with increasing protein lysate demonstrated linearity with the spectrophotometric assay. Furthermore, the assay detected at least 2 µg changes in protein quantity with short incubation times. The saturation curve for A-1-TG hydrolysis demonstrates that this reaction follows Michaelis-Menten kinetics. Hydrolytic activity was equally divided between membrane and cytosolic fractions, which is characteristic of peripheral membrane proteins. It showed a total loss of enzyme activity when catalytic serine of MAGL was mutated to an alanine.

These results are comparable to those obtained with radiometric assays in previous studies. The K_m of 67.9 ± 26.1 calculated with the spectrophotometric assay was nearly identical to the K_m of 67.8 ± 4.0 µM determined for rat cerebellar membranes using a radiometric assay (Saario et al., 2004). Muccioli and colleagues also determined that MAGL activity was not significantly different between membrane and cytosolic fractions when compared to total cell lysate activity (Muccioli et al., 2007). Initial studies showed MAGL possessed a catalytic triad characteristic of serine hydrolases. Subsequent mutation of serine 122 to an alanine abolished enzyme activity showing that this residue is essential for catalysis (Karlsson et al., 1997). This result was duplicated with the spectrophotometric assay.

The sensitivity and precision of the spectrophotometric assay was compared to a radiometric assay through inhibition studies. The colorimetric assay could not detect inhibition at the lowest concentration of NAM used and generally showed higher percent remaining activity with all NAM concentrations examined when compared with the radiometric assay. However, the spectrophotometric assay was found to be as precise as the radiometric assay.

Other alternative assays have been previously developed. One colorimetric assay used 4-nitrophenylacetate to quantify MAGL activity with V_{max} = 52.2 µmol/min/mg (Muccioli et al., 2008). A second assay utilized the fluoregenic substrate 7-hydroxycoumarinyl-arachidonate with V_{max} = 1700 µmol/min/mg (Wang et al., 2008). Both these methods obtained results comparable to radiometric assays. The fluorescent

assay was intended for use with purified MAGL while the assay using 4-nitrophenylacetate as well as the assay described herein have the advantage of working with homogenates and do not require a spectrofluorimeter or scintillation counter. The rates of hydrolysis for the various substrates vary widely. This is owing to their specific structure and the resulting susceptibility to hydrolysis by MAGL and the purity of the MAGL preparations. Conveniently, the substrate (A-1-TG) used in the current study is hydrolyzed at approximately a 10-fold rate relative to the radioactive substrate (^{3}H-2-OG).

The spectrophotometric assay described here was useful for measuring linear increases in activity with an increase in MAGL-transfected cell lysate protein, MAGL kinetics, and distribution of enzyme activity in cellular fractions. Although not as sensitive as a radiometric assay, NAM inhibition of MAGL was detectable except at the lowest concentration of inhibitor. Loss of total activity in a catalytic mutant was also detectable. The assay can be used with both purified MAGL or cultured cells.

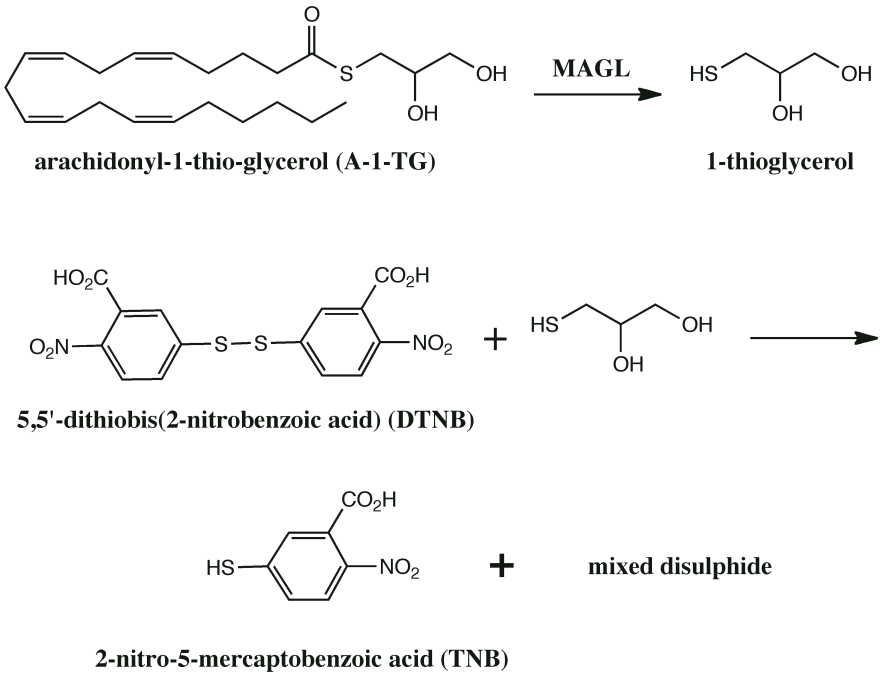

Figure 15. Scheme for arachidonoyl-1-thio-glycerol hydrolysis and the subsequent color reaction. Arachidonoyl-1-thio-glycerol is hydrolyzed by MAGL releasing a thioglycerol. The thioglycerol reacts with DTNB relasing the yellow-colored ion, TNB.

A

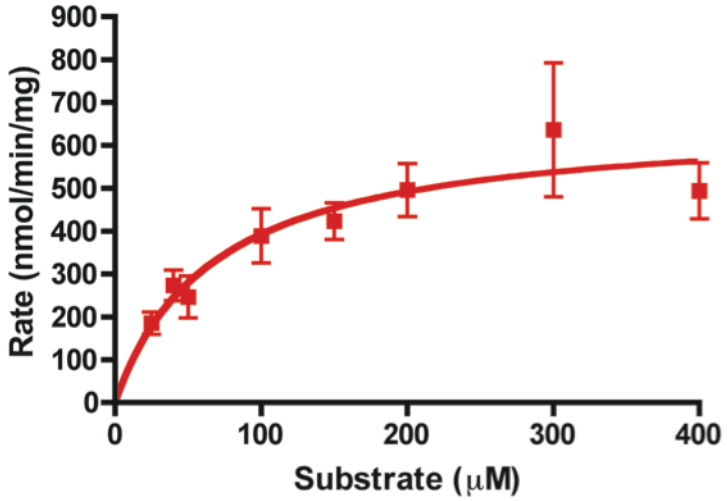

B

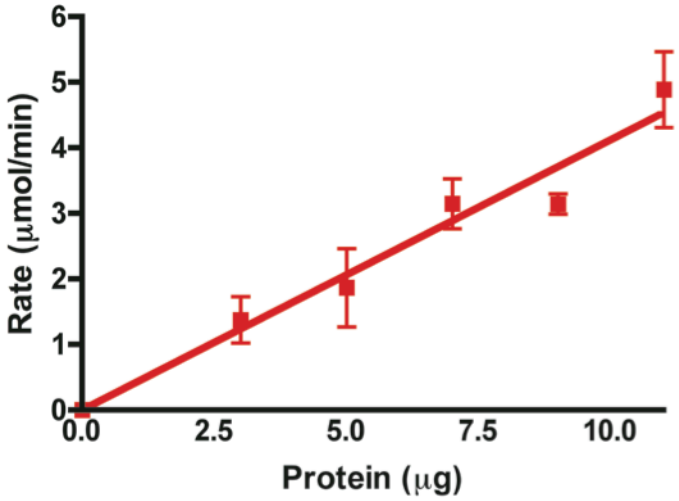

Figure 16. Test for linearity (A) and MIchaelis-Menten Kinetics (B) for hydrolysis of arachidonoyl-1-thio-glycerol. (A) Arachidonoyl-1-thio-glycerol (200 μM) was incubated with increasing amounts of lysate protein (3-11 μg) from transiently transfected COS-7 cells for 3 min. at 37°C. (**B)** Five micrograms lysate protein from transiently transfected COS-7 was incubated with increasing concentrations of arachidonoyl-1-thio-glycerol (25-400 μM) for 5 min. at 37°C. The reaction mix plus 400 nM MAFP was used the negative control. Values are reported as mean±SEM (n=3).

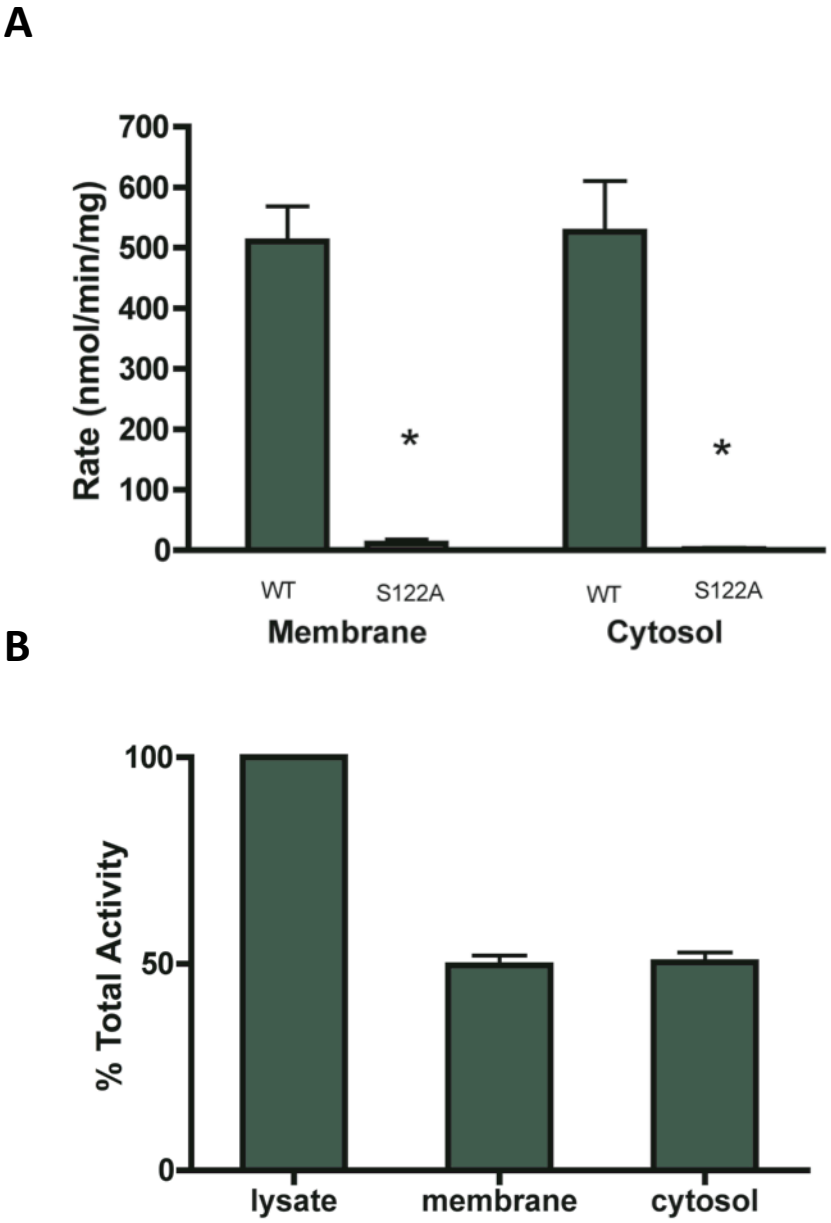

Figure 17. Activity of MAGL (A) and MAGL122A (B) in cellular fractions. (A) Seven micrograms protein from each COS-7 cell fraction was incubated with 70 μM arachidonoyl-1-thioglycerol for 3 min. at 37°C. (**B)** Catalytic Ser-122 of MAGL was mutated to an alanine. Experiments as described in **A** were repeated with COS-7 cells transiently transfected with this mutant. Activity of mutant (starred column) was compared to wild-type (green column) activity. The reaction mix plus 500 nM MAFP was used as the negative control. Values are reported as the mean±SEM (n=3, *P<0.0001).

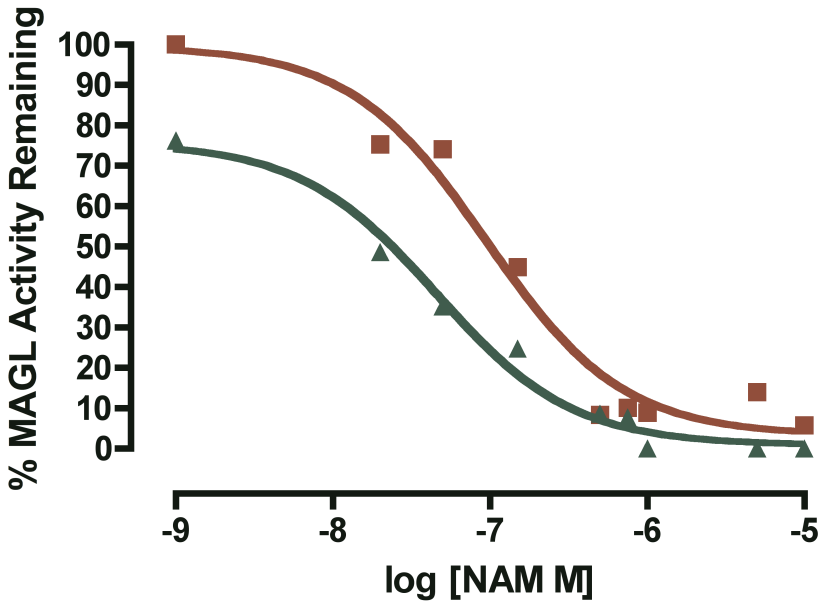

Figure 18. Inhibition of MAGL by NAM using arachidonoyl-1-thio-glycerol (spectrophotometric) or ^{3}H-2-oleoylglycerol (radiometric). Ten micrograms lysate protein from transiently transfected COS-7 cells was pre-incubated with increasing amounts of NAM (1 nM – 10 μM) and then incubated with either arachidonoyl-1-thiolgycerol (70 μM) (filled square) or ^{3}H-2-oleoylglycerol (15,000 cpm) (filled upright triangle). Shown here are results for a typical experiment. Boiled COS-7 cell lysate activity was substracted from raw data to account for background.

REFERENCES

Batkai, S., and Pacher, P. (2009). Endocannabinoids and cardiac contractile function: pathophysiological implications. Pharmacol Res *60*, 99-106.

Beltramo, M., and Piomelli, D. (2000). Carrier-mediated transport and enzymatic hydrolysis of the endogenous cannabinoid 2-arachidonylglycerol. Neuroreport *11*, 1231-1235.

Berdyshev, E.V. (2000). Cannabinoid receptors and the regulation of immune response. Chem Phys Lipids *108*, 169-190.

Bertrand, T., Auge, F., Houtmann, J., Rak, A., Vallee, F., Mikol, V., Berne, P.F., Michot, N., Cheuret, D., Hoornaert, C*., et al.* (2010). Structural basis for human monoglyceride lipase inhibition. J Mol Biol *396*, 663-673.

Blankman, J.L., Simon, G.M., and Cravatt, B.F. (2007). A comprehensive profile of brain enzymes that hydrolyze the endocannabinoid 2-arachidonoylglycerol. Chem Biol *14*, 1347-1356.

Chakrabarti, A., Onaivi, E.S., and Chaudhuri, G. (1995). Cloning and sequencing of a cDNA encoding the mouse brain-type cannabinoid receptor protein. DNA Seq *5*, 385-388.

Chau, L.Y., and Tai, H.H. (1988). Monoglyceride and diglyceride lipases from human platelet microsomes. Biochim Biophys Acta *963*, 436-444.

Chen, H., and De Camilli, P. (2005). The association of epsin with ubiquitinated cargo along the endocytic pathway is negatively regulated by its interaction with clathrin. Proc Natl Acad Sci U S A *102*, 2766-2771.

Cheng, A., Bollan, K.A., Greenwood, S.M., Irving, A.J., and Connolly, C.N. (2007). Differential subcellular localization of RIC-3 isoforms and their role in determining 5-HT3 receptor composition. J Biol Chem *282*, 26158-26166.

Devane, W.A., Dysarz, F.A., 3rd, Johnson, M.R., Melvin, L.S., and Howlett, A.C. (1988). Determination and characterization of a cannabinoid receptor in rat brain. Mol Pharmacol *34*, 605-613.

Devane, W.A., Hanus, L., Breuer, A., Pertwee, R.G., Stevenson, L.A., Griffin, G., Gibson, D., Mandelbaum, A., Etinger, A., and Mechoulam, R. (1992). Isolation and structure of a brain constituent that binds to the cannabinoid receptor. Science *258*, 1946-1949.

Dinh, T.P., Carpenter, D., Leslie, F.M., Freund, T.F., Katona, I., Sensi, S.L., Kathuria, S., and Piomelli, D. (2002). Brain monoglyceride lipase participating in endocannabinoid inactivation. Proc Natl Acad Sci U S A *99*, 10819-10824.

Dinh, T.P., Kathuria, S., and Piomelli, D. (2004). RNA interference suggests a primary role for monoacylglycerol lipase in the degradation of the endocannabinoid 2-arachidonoylglycerol. Mol Pharmacol *66*, 1260-1264.

Fiskerstrand, T., H'Mida-Ben Brahim, D., Johansson, S., M'Zahem, A., Haukanes, B.I., Drouot, N., Zimmermann, J., Cole, A.J., Vedeler, C., Bredrup, C*., et al.* (2010). Mutations in ABHD12 cause the neurodegenerative disease PHARC: An inborn error of endocannabinoid metabolism. Am J Hum Genet *87*, 410-417.

Fowler, C.J., Rojo, M.L., and Rodriguez-Gaztelumendi, A. (2010). Modulation of the endocannabinoid system: neuroprotection or neurotoxicity? Exp Neurol *224*, 37-47.

Fredrikson, G., Tornqvist, H., and Belfrage, P. (1986). Hormone-sensitive lipase and monoacylglycerol lipase are both required for complete degradation of adipocyte triacylglycerol. Biochim Biophys Acta *876*, 288-293.

Fride, E. (2005). Endocannabinoids in the central nervous system: from neuronal networks to behavior. Curr Drug Targets CNS Neurol Disord *4*, 633-642.

Gao, Y., Vasilyev, D.V., Goncalves, M.B., Howell, F.V., Hobbs, C., Reisenberg, M., Shen, R., Zhang, M.Y., Strassle, B.W., Lu, P.*, et al.* (2010). Loss of retrograde endocannabinoid signaling and reduced adult neurogenesis in diacylglycerol lipase knock-out mice. J Neurosci *30*, 2017-2024.

Gaoni, Y., R. Mechoulam (1964). Isolation, structure and partial synthesis of an active constituent of hashish. J Am Chem Soc *86*, 1646-1647.

Gerard, C., Mollereau, C., Vassart, G., and Parmentier, M. (1990). Nucleotide sequence of a human cannabinoid receptor cDNA. Nucleic Acids Res *18*, 7142.

Goparaju, S.K., Ueda, N., Taniguchi, K., and Yamamoto, S. (1999). Enzymes of porcine brain hydrolyzing 2-arachidonoylglycerol, an endogenous ligand of cannabinoid receptors. Biochem Pharmacol *57*, 417-423.

Goparaju, S.K., Ueda, N., Yamaguchi, H., and Yamamoto, S. (1998). Anandamide amidohydrolase reacting with 2-arachidonoylglycerol, another cannabinoid receptor ligand. FEBS Lett *422*, 69-73.

Gulyas, A.I., Cravatt, B.F., Bracey, M.H., Dinh, T.P., Piomelli, D., Boscia, F., and Freund, T.F. (2004). Segregation of two endocannabinoid-hydrolyzing enzymes into pre- and postsynaptic compartments in the rat hippocampus, cerebellum and amygdala. Eur J Neurosci *20*, 441-458.

Hashimotodani, Y., Ohno-Shosaku, T., Tsubokawa, H., Ogata, H., Emoto, K., Maejima, T., Araishi, K., Shin, H.S., and Kano, M. (2005). Phospholipase Cbeta serves as a coincidence detector through its Ca2+ dependency for triggering retrograde endocannabinoid signal. Neuron *45*, 257-268.

Heckman, K.L., and Pease, L.R. (2007). Gene splicing and mutagenesis by PCR-driven overlap extension. Nat Protoc *2*, 924-932.

Hohmann, A.G., and Suplita, R.L., 2nd (2006). Endocannabinoid mechanisms of pain modulation. AAPS J *8*, E693-708.

Howlett, A.C., Johnson, M.R., Melvin, L.S., and Milne, G.M. (1988). Nonclassical cannabinoid analgetics inhibit adenylate cyclase: development of a cannabinoid receptor model. Mol Pharmacol *33*, 297-302.

Kano, M., Ohno-Shosaku, T., Hashimotodani, Y., Uchigashima, M., and Watanabe, M. (2009). Endocannabinoid-mediated control of synaptic transmission. Physiol Rev *89*, 309-380.

Karlsson, M., Contreras, J.A., Hellman, U., Tornqvist, H., and Holm, C. (1997). cDNA cloning, tissue distribution, and identification of the catalytic triad of monoglyceride lipase. Evolutionary relationship to esterases, lysophospholipases, and haloperoxidases. J Biol Chem *272*, 27218-27223.

Karlsson, M., Reue, K., Xia, Y.R., Lusis, A.J., Langin, D., Tornqvist, H., and Holm, C. (2001). Exon-intron organization and chromosomal localization of the mouse monoglyceride lipase gene. Gene *272*, 11-18.

King, A.R., Lodola, A., Carmi, C., Fu, J., Mor, M., and Piomelli, D. (2009). A critical cysteine residue in monoacylglycerol lipase is targeted by a new class of isothiazolinone-based enzyme inhibitors. Br J Pharmacol *157*, 974-983.

Kreitzer, A.C., and Regehr, W.G. (2001). Retrograde inhibition of presynaptic calcium influx by endogenous cannabinoids at excitatory synapses onto Purkinje cells. Neuron *29*, 717-727.

Labar, G., Bauvois, C., Borel, F., Ferrer, J.L., Wouters, J., and Lambert, D.M. (2010). Crystal structure of the human monoacylglycerol lipase, a key actor in endocannabinoid signaling. Chembiochem *11*, 218-227.

Lang, W., Qin, C., Lin, S., Khanolkar, A.D., Goutopoulos, A., Fan, P., Abouzid, K., Meng, Z., Biegel, D., and Makriyannis, A. (1999). Substrate Specificity and Stereoselectivity of Rat Brain Microsomal Anandamide Amidohydrolase. J Med Chem *42*, 1682.

Lehto, M., Hynynen, R., Karjalainen, K., Kuismanen, E., Hyvarinen, K., and Olkkonen, V.M. (2005). Targeting of OSBP-related protein 3 (ORP3) to endoplasmic reticulum and plasma membrane is controlled by multiple determinants. Exp Cell Res *310*, 445-462.

Li, C., Jones, P.M., and Persaud, S.J. (2011). Role of the endocannabinoid system in food intake, energy homeostasis and regulation of the endocrine pancreas. Pharmacol Ther *129*, 307-320.

Long, J.Z., Nomura, D.K., and Cravatt, B.F. (2009). Characterization of monoacylglycerol lipase inhibition reveals differences in central and peripheral endocannabinoid metabolism. Chem Biol *16*, 744-753.

Ludanyi, A., Hu, S.S., Yamazaki, M., Tanimura, A., Piomelli, D., Watanabe, M., Kano, M., Sakimura, K., Magloczky, Z., Mackie, K.*, et al.* (2011). Complementary synaptic distribution of enzymes responsible for synthesis and inactivation of the endocannabinoid 2-arachidonoylglycerol in the human hippocampus. Neuroscience *174*, 50-63.

Maejima, T., Hashimoto, K., Yoshida, T., Aiba, A., and Kano, M. (2001). Presynaptic inhibition caused by retrograde signal from metabotropic glutamate to cannabinoid receptors. Neuron *31*, 463-475.

Maejima, T., Oka, S., Hashimotodani, Y., Ohno-Shosaku, T., Aiba, A., Wu, D., Waku, K., Sugiura, T., and Kano, M. (2005). Synaptically driven endocannabinoid release requires Ca2+-assisted metabotropic glutamate receptor subtype 1 to phospholipase Cbeta4 signaling cascade in the cerebellum. J Neurosci *25*, 6826-6835.

Mailleux, P., Parmentier, M., and Vanderhaeghen, J.J. (1992). Distribution of cannabinoid receptor messenger RNA in the human brain: an in situ hybridization histochemistry with oligonucleotides. Neurosci Lett *143*, 200-204.

Marrs, W.R., Blankman, J.L., Horne, E.A., Thomazeau, A., Lin, Y.H., Coy, J., Bodor, A.L., Muccioli, G.G., Hu, S.S., Woodruff, G.*, et al.* (2010). The serine hydrolase ABHD6 controls the accumulation and efficacy of 2-AG at cannabinoid receptors. Nat Neurosci *13*, 951-957.

Matsuda, D., and Mauro, V.P. (2010). Determinants of initiation codon selection during translation in mammalian cells. PLoS One *5*, e15057.

Matsuda, L.A., Bonner, T.I., and Lolait, S.J. (1993). Localization of cannabinoid receptor mRNA in rat brain. J Comp Neurol *327*, 535-550.

Matsuda, L.A., Lolait, S.J., Brownstein, M.J., Young, A.C., and Bonner, T.I. (1990). Structure of a cannabinoid receptor and functional expression of the cloned cDNA. Nature *346*, 561-564.

Mechoulam, R., Ben-Shabat, S., Hanus, L., Ligumsky, M., Kaminski, N.E., Schatz, A.R., Gopher, A., Almog, S., Martin, B.R., Compton, D.R.*, et al.* (1995). Identification of an endogenous 2-monoglyceride, present in canine gut, that binds to cannabinoid receptors. Biochem Pharmacol *50*, 83-90.

Mechoulam, R., Shani, A., Edery, H., and Grunfeld, Y. (1970). Chemical basis of hashish activity. Science *169*, 611-612.

Muccioli, G.G., Labar, G., and Lambert, D.M. (2008). CAY10499, a novel monoglyceride lipase inhibitor evidenced by an expeditious MGL assay. Chembiochem *9*, 2704-2710.

Muccioli, G.G., Xu, C., Odah, E., Cudaback, E., Cisneros, J.A., Lambert, D.M., Lopez Rodriguez, M.L., Bajjalieh, S., and Stella, N. (2007). Identification of a novel endocannabinoid-hydrolyzing enzyme expressed by microglial cells. J Neurosci *27*, 2883-2889.

Munro, S., Thomas, K.L., and Abu-Shaar, M. (1993). Molecular characterization of a peripheral receptor for cannabinoids. Nature *365*, 61-65.

Ohno-Shosaku, T., Maejima, T., and Kano, M. (2001). Endogenous cannabinoids mediate retrograde signals from depolarized postsynaptic neurons to presynaptic terminals. Neuron *29*, 729-738.

Patricelli, M.P., and Cravatt, B.F. (1999). Fatty acid amide hydrolase competitively degrades bioactive amides and esters through a nonconventional catalytic mechanism. Biochemistry *38*, 14125-14130.

Pisanti, S., and Bifulco, M. (2009). Endocannabinoid system modulation in cancer biology and therapy. Pharmacol Res *60*, 107-116.

Riddles, P.W., Blakeley, R.L., and Zerner, B. (1983). Reassessment of Ellman's reagent. Methods Enzymol *91*, 49-60.

Saario, S.M., and Laitinen, J.T. (2007). Monoglyceride lipase as an enzyme hydrolyzing 2-arachidonoylglycerol. Chem Biodivers *4*, 1903-1913.

Saario, S.M., Salo, O.M., Nevalainen, T., Poso, A., Laitinen, J.T., Jarvinen, T., and Niemi, R. (2005). Characterization of the sulfhydryl-sensitive site in the enzyme responsible for hydrolysis of 2-arachidonoyl-glycerol in rat cerebellar membranes. Chem Biol *12*, 649-656.

Saario, S.M., Savinainen, J.R., Laitinen, J.T., Jarvinen, T., and Niemi, R. (2004). Monoglyceride lipase-like enzymatic activity is responsible for hydrolysis of 2-arachidonoylglycerol in rat cerebellar membranes. Biochem Pharmacol *67*, 1381-1387.

Schalk-Hihi, C., Schubert, C., Alexander, R., Bayoumy, S., Clemente, J.C., Deckman, I., DesJarlais, R.L., Dzordzorme, K.C., Flores, C.M., Grasberger, B.*, et al.* (2011). Crystal structure of a soluble form of human monoglyceride lipase in complex with an inhibitor at 1.35 A resolution. Protein Sci *20*, 670-683.

Schlosburg, J.E., Blankman, J.L., Long, J.Z., Nomura, D.K., Pan, B., Kinsey, S.G., Nguyen, P.T., Ramesh, D., Booker, L., Burston, J.J.*, et al.* (2010). Chronic monoacylglycerol lipase blockade causes functional antagonism of the endocannabinoid system. Nat Neurosci *13*, 1113-1119.

Snapp, E.L., Hegde, R.S., Francolini, M., Lombardo, F., Colombo, S., Pedrazzini, E., Borgese, N., and Lippincott-Schwartz, J. (2003). Formation of stacked ER cisternae by low affinity protein interactions. J Cell Biol *163*, 257-269.

Steinberg, S.F. (2008). Structural basis of protein kinase C isoform function. Physiol Rev *88*, 1341-1378.

Straiker, A., Hu, S.S., Long, J.Z., Arnold, A., Wager-Miller, J., Cravatt, B.F., and Mackie, K. (2009). Monoacylglycerol lipase limits the duration of endocannabinoid-mediated depolarization-induced suppression of excitation in autaptic hippocampal neurons. Mol Pharmacol *76*, 1220-1227.

Straiker, A., and Mackie, K. (2009). Cannabinoid signaling in inhibitory autaptic hippocampal neurons. Neuroscience *163*, 190-201.

Straiker, A., Wager-Miller, J., Hu, S.S., Blankman, J.L., Cravatt, B.F., and Mackie, K. (2011). COX-2 and FAAH can regulate the time course of depolarization induced suppression of excitation. Br J Pharmacol.

Sugiura, T., Kobayashi, Y., Oka, S., and Waku, K. (2002). Biosynthesis and degradation of anandamide and 2-arachidonoylglycerol and their possible physiological significance. Prostaglandins Leukot Essent Fatty Acids *66*, 173-192.

Sugiura, T., Kondo, S., Sukagawa, A., Nakane, S., Shinoda, A., Itoh, K., Yamashita, A., and Waku, K. (1995). 2-Arachidonoylglycerol: a possible endogenous cannabinoid receptor ligand in brain. Biochem Biophys Res Commun *215*, 89-97.

Tanasescu, R., and Constantinescu, C.S. (2010). Cannabinoids and the immune system: an overview. Immunobiology *215*, 588-597.

Tanimura, A., Yamazaki, M., Hashimotodani, Y., Uchigashima, M., Kawata, S., Abe, M., Kita, Y., Hashimoto, K., Shimizu, T., Watanabe, M.*, et al.* (2010). The endocannabinoid 2-arachidonoylglycerol produced by diacylglycerol lipase alpha mediates retrograde suppression of synaptic transmission. Neuron *65*, 320-327.

Thakur, G.A., Nikas, S.P., and Makriyannis, A. (2005). CB1 cannabinoid receptor ligands. Mini Rev Med Chem *5*, 631-640.

Tornqvist, H., and Belfrage, P. (1976). Purification and some properties of a monoacylglycerol-hydrolyzing enzyme of rat adipose tissue. J Biol Chem *251*, 813-819.

Turu, G., and Hunyady, L. (2010). Signal transduction of the CB1 cannabinoid receptor. J Mol Endocrinol *44*, 75-85.

Walker, J.M., and Huang, S.M. (2002). Endocannabinoids in pain modulation. Prostaglandins Leukot Essent Fatty Acids *66*, 235-242.

Wang, Y., Chanda, P., Jones, P.G., and Kennedy, J.D. (2008). A fluorescence-based assay for monoacylglycerol lipase compatible with inhibitor screening. Assay Drug Dev Technol *6*, 387-393.

Wilson, R.I., and Nicoll, R.A. (2001). Endogenous cannabinoids mediate retrograde signalling at hippocampal synapses. Nature *410*, 588-592.

Zvonok, N., Pandarinathan, L., Williams, J., Johnston, M., Karageorgos, I., Janero, D.R., Krishnan, S.C., and Makriyannis, A. (2008). Covalent inhibitors of human monoacylglycerol lipase: ligand-assisted characterization of the catalytic site by mass spectrometry and mutational analysis. Chem Biol *15*, 854-862.